Figure 5. Hematopoietic differentiation from HE is inhibited by depletion of SOX17. (A) Knock-down efficiencies of shRNAs against *SOX17*. Western blot analysis of SOX17 in 293T cells transduced with shRNAs against *SOX17* (top panel). α-Tubulin was used as the loading control. pre-HPCs from day 8 EBs were transduced with shRNAs against *SOX17* on OP9 cells and cultured in the presence of 20 ng/mL of SCF and TPO, 10 ng/mL of IL-3, and 3 units/mL of erythropoietin (EPO) for 7 days. Levels of endogenous *SOX17* were analyzed by quantitative RT-PCR analysis (bottom panel). mRNA levels were normalized to *GAPDH* expression. Expression levels relative to that in the control cells transduced with an shRNA against *Luciferase* are shown as the means ± SD for triplicate analyses. (B) Effects of depletion of SOX17 on hematopoietic development from HE cells. ECs from day 5 EBs were transduced with shRNAs against *SOX17* on OP9 cells and were cultured in the presence of 20 ng/mL of SCF and TPO, 10 ng/mL of IL-3, and 3 units/mL of EPO for 9 days. Representative flow cytometric profiles of cells at day 9 of culture are depicted. (C) Absolute numbers and proportion of CD235a$^+$ erythroblasts and CD11b$^+$ myeloid cells in panel B at day 9 of culture. Data are shown as the means ± SD for 3 independent cultures. (D) Effects of depletion of SOX17 on pre-HPCs. Pre-HPCs from day 8 EBs were transduced with shRNAs against *SOX17* on OP9 cells and were cultured in the presence of 20 ng/mL of SCF and TPO, 10 ng/mL of IL-3, and 3 units/mL of EPO for 7 days. Absolute numbers and proportion of CD235a$^+$ erythroblasts and CD11b$^+$ myeloid cells at day 7 of culture are presented. Data are shown as the means ± SD for triplicate cultures of 1 of 2 independent experiments that gave similar results.

SOX17 regulates directly the transcription of key regulator genes for HE cells

A ChIP-on-chip analysis was conducted to identify the direct target genes of SOX17 in HE cells. We transduced ECs cells from day 6 EBs with a *3xFlag-Sox17-ERT* retrovirus and expanded CD34$^+$CD43$^+$CD45$^{-/low}$ HE-like cells on OP9 cells. At day 27 of culture, 94.2% of the expanded cells were positive for CD34. CD34$^+$ cells were further enriched (99.8%) by magnetic cell sorting using magnetic beads conjugated with anti-CD34 Abs, and these purified cells were then subjected to ChIP-on-chip analysis.

The ChIP-on-chip analysis was performed with human promoter microarrays containing approximately 21 000 probe sets covering from −8.0 kb upstream to +4.0 kb downstream of the TSS of RefSeq genes. 3xFlag-Sox17 was cross-linked to DNA and precipitated using the anti-FLAG M2 Ab. Gene promoters bound by Sox17 were ranked according to fold enrichments calculated in comparison with signals obtained with the input DNA. Of the

19 457 gene promoter regions analyzed, 182 and 98 regions showed Sox17 binding with an enrichment greater than 2- and 3-fold, respectively (full data are listed in supplemental Table 2). The functional annotation of the genes bound by Sox17 with a fold enrichment greater than 3 was performed based on GO and showed significant enrichment for genes that fell into categories such as "vasculogenesis," "hemopoiesis," and "positive regulation of erythrocyte differentiation" (Figure 6A, Table 1, and supplemental Table 2). The genes bound by Sox17 include genes well characterized as regulators of hematopoietic development from HE cells, such as *VE-cadherin/CDH5*, *RUNX1*, *SCL/TAL1*, and *HHEX* (Table 1 and supplemental Table 2). VE-cadherin, an endothelial marker antigen, is expressed by HE cells and by early HSCs, which appear in the yolk sac and the aorta-gonad-mesonephros region, as well as by a transient HSC population of the fetal liver.[23-25] *RUNX1*, *SCL/TAL1*, and *HHEX* encode transcription factors essential for the development of HSCs from HE cells or hemangioblasts.[5,26,27] The

Figure 6. Targets of SOX17 detected by ChIP-on-chip analysis. (A) GO analysis of the Sox17 targets detected by ChIP-on-chip analysis. CD34⁺CD43⁻ cells from day 6 EBs were transduced with a 3× Flag *SOX17-ERT* retrovirus. The cells were further cultured on OP9 cells in the presence of 20 ng/mL of SCF and TPO and 200nM 4-OHT. CD34⁺ cells were collected at day 27 of culture and subjected to ChIP-on-chip analysis. *P* for each GO term is indicated. (B) ChIP-on-chip profile of SOX17 occupancy at genes related to hematopoietic development from HE cells. Plot under the x-axis shows the position of probe sets. Arrowhead at the *VE-cadherin/CDH5* promoter indicate consensus motif of Sox17-binding site. (C) Gene-expression patterns of wild-type and engineered cells obtained in microarray analyses clustered using hierarchical clustering. Distance between 2 samples was defined with the Pearson correlation of Sox17 target genes with Sox17 binding more than 3-fold in the ChIP-on-chip analysis presented in supplemental Table 2. The color of each cell represents the value of correlation indicated on the right side of the matrix. (D) Comparative analysis of ChIP-on-chip and microarray data. Venn diagrams showing the number of genes bound by Sox17 (> 3-fold enrichment) and the number of genes up-regulated in expression more than 2-fold in at least 1 cell type among ECs, pre-HPCs, and HPCs on overexpression of *Sox17* (*Sox17*-overexpressing CD34⁺CD43⁺CD45⁻/low cells compared with those of respective fresh controls; left panel). The percentages of overlapping and nonoverlapping bound genes are indicated in parentheses. Shown are the correlation of Sox17 binding (fold enrichment) in ChIP-on-chip analysis and the fold changes in expression during differentiation of ECs to HPCs (right panel). The fold enrichments and fold changes in expression were plotted for 84 genes of 98 showing enrichments greater than 3-fold (the microarray data were not available for the remaining 14 genes). Correlation coefficients (R) are indicated for genes with fold enrichment greater than 3- and 6-fold, respectively.
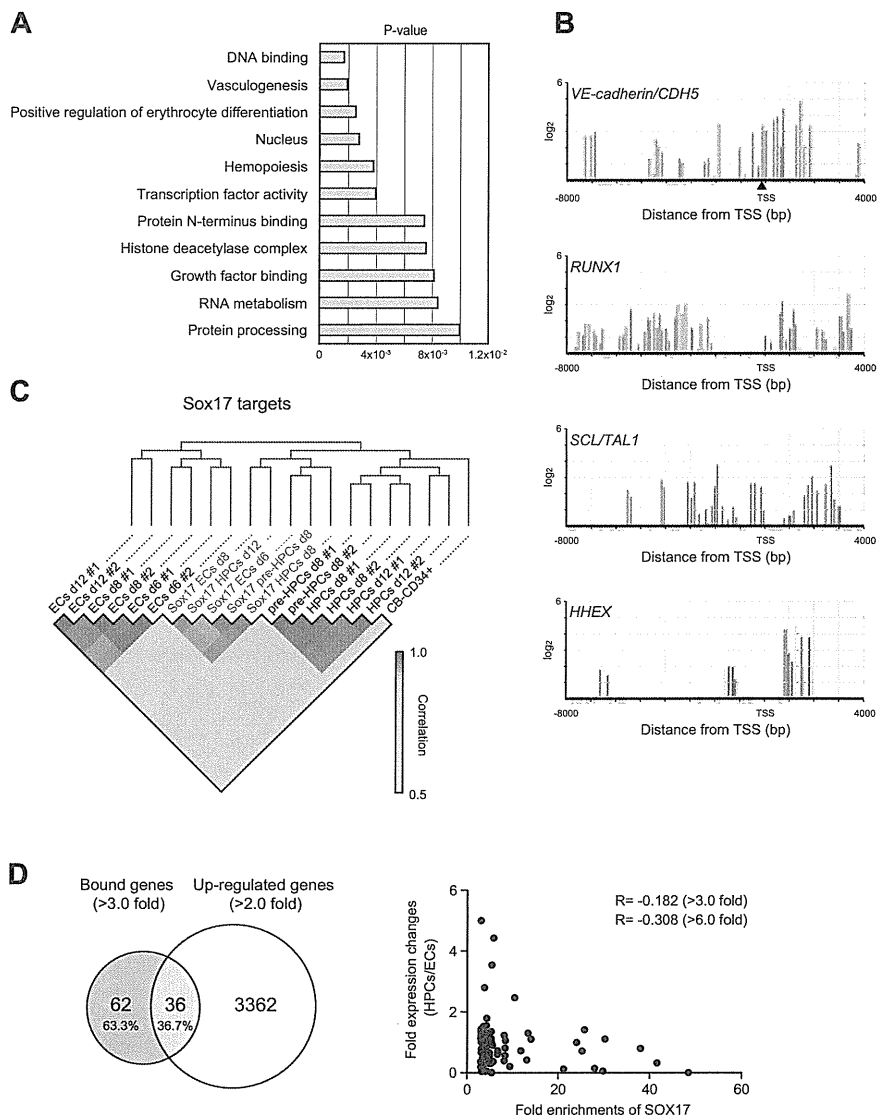
distribution of SOX17 signals at these genes varied greatly across the promoter region (Figure 6B). SOX17 is reported to bind to the consensus motif of "ATTGT."[22] The *VE-cadherin/CDH5* promoter contains the consensus motif between −107 bp and −103 bp from the TSS. It was recently reported that this site is conserved in mouse and Sox7 binds directly to it to activate transcription.[28] Our ChIP-on-chip data showed that Sox17 binds to this site as well (Figure 6B arrowhead). These findings clearly indicate that SOX17 regulates directly the expression of a set of key genes for hematopoietic development in HE cells.

We next performed hierarchical clustering of the cell populations based on the microarray data using "SOX17 targets" that we arbitrarily selected as genes with Sox17 binding greater than 3-fold over the input levels in the ChIP-on-chip analysis (supplemental Table 2). As expected, *Sox17*-overexpressing cells were again developmentally placed between ECs and pre-HPCs/HPCs (Figure 6C).

Comparison of gene lists between the ChIP-on-chip and microarray assays

We next examined the changes in expression of the 98 genes bound by Sox17 (> 3-fold enrichment in the ChIP-on-chip analysis) on *Sox17* overexpression. The microarray data of *Sox17*-overexpressing CD34⁺CD43⁺CD45⁻/low cells shown in Figure 3 were compared with those of respective fresh controls. Sox17 is thought to activate the transcription of target genes.[22] As expected, 36 of the 98 genes showed up-regulation in expression of more than 2-fold in at least in 1 cell type (Figure 6D, Table 1, and supplemental Table 2). This tendency was evident in the top 15 genes with Sox17 binding (Table 1 and supplemental Table 2), although in 4 genes of 15, the effects of overexpression of *Sox17* were obvious only in pre-HPCs and HPCs, but not in ECs, which possess a high level of endogenous SOX17 (supplemental Table 2). Similarly, a negative correlation was detected between the levels of Sox17 binding in ChIP-on-chip analysis and the fold changes in expression during differentiation of ECs (SOX17⁺) to HPCs (SOX17⁻; Figure 6D). Among genes bound by Sox17, *EGFL7* and *VE-cadherin/CDH5* have been shown to be up-regulated in BM HPCs transduced with *Sox17*.[13] However, in our ChIP-on-chip analysis, Sox17 did not show any binding to the genes directly regulated by Sox17 during differentiation of ES cells into extraembryonic endoderm.[22] These data suggest that SOX17 regulates different targets in hematopoietic and endodermal development.

— 187 —

Table 1. Candidate SOX17 target genes according to ChIP-chip scores

Rank	Symbol	Gene name	Fold enrichment	GO term			Fold difference		
				Vasculogenesis	Positive regulation of erythrocyte differentiation	Hemopoiesis	Sox17 ECs d6/ECs d6	Sox17 pre-HPCs d8/pre-HPCs d8	Sox17 HPCs d8/HPCs d8
1	GPSM3	G-protein signaling modulator 3	48.50	No	No	No	1.38	2.42	2.56
2	MAST4	Microtubule associated serine/threonine kinase family member 4	41.62	No	No	No	1.02	3.22	4.75
3	TXLNB	Taxilin beta, muscle-derived protein 77	38.05	No	No	No	1.18	2.89	4.29
4	EGOT	Eosinophil granule ontogeny transcript	37.53	No	No	No	ND	ND	ND
5	PPBPL1	Pro-platelet basic protein-like 1	35.26	No	No	No	ND	ND	ND
6	MFSD6	Major facilitator superfamily domain containing 6	30.27	No	No	No	19.79	14.24	19.26
7	CDH5	Cadherin 5, type 2	29.86	No	No	No	0.70	9.07	10.81
8	BCL6B	B-cell CLL/lymphoma 6, member B	28.05	No	No	No	1.11	5.73	8.50
9	C1orf55	Chromosome 1 open reading frame 55	25.81	No	No	No	2.23	1.77	1.44
10	PTTG1IP	Pituitary tumor-transforming 1 interacting protein	25.28	No	No	No	0.93	1.49	1.67
11	TRIM67	Tripartite motif containing 67	24.08	No	No	No	4.16	4.29	5.03
12	MYCT1	myc target 1myc target 1	21.26	No	No	No	0.74	2.90	7.66
13	CD40LG	CD40 ligand	14.12	No	No	No	6.65	11.57	16.69
14	SCOC	Short coiled-coil protein	13.45	No	No	No	0.97	0.79	1.04
15	PPP1R16B	Protein phosphatase 1, regulatory subunit 16B	13.18	No	No	No	0.70	1.83	1.15
19	ACVR2A	Activin A receptor, type IIA	9.45	No	Yes	No	0.15	0.42	0.67
26	HHEX	Hematopoietically expressed homeobox	6.87	Yes	No	Yes	0.66	1.44	0.89
37	RUNX1	runt-related transcription factor 1	5.46	No	No	Yes	5.02	1.25	1.12
41	TAL1/SCL	T-cell acute lymphocytic leukemia 1	5.28	No	Yes	Yes	1.82	1.76	1.92
50	EGFL7	EGF-like-domain, multiple 7	4.69	Yes	No	No	0.67	2.11	1.92
69	JUNB	jun B protooncogene	3.78	Yes	No	No	3.50	3.87	3.24

ND indicates no data.

Discussion

In the present study, we found that all of the *SOXF* subfamily genes, *SOX7*, *SOX17*, and *SOX18*, are highly expressed in hESC-derived ECs enriched in HE and markedly down-regulated in pre-HPCs and HPCs to the levels comparable to that in CB CD34+ cells. Overexpression of *Sox17* in ECs resulted in expansion of monotonous cells with a CD34+CD43+CD45−/low immunophenotype. These cells coexpressed hematopoietic marker antigens such as CD43 and a low level of CD45, as well as the HE marker VE-cadherin. These unique characteristics of *Sox17*-overexpressing ECs are reminiscent of HE cells. Overexpression of *Sox17* inhibited the hematopoietic differentiation of both pre-HPCs and HPCs and reprogrammed them into HE-like cells. In contrast, depletion of *SOX17* in pre-HPCs did not affect their hematopoietic differentiation. These findings suggest that SOX17 is one of the master regulators that define HE but must be down-regulated during the development of pre-HPCs to allow hematopoietic differentiation.

The effects of overexpression of *SOX17* in hESC-derived ECs and HPCs are very similar to that of overexpression of *Sox7* and *Sox18* in early hematopoietic precursors from mouse embryos and mouse ESCs.[14,15,28] However, it has been reported in mice that *Sox17* remains marginally expressed during blood specification and the overexpression of *Sox17* in early hematopoietic precursors induces massive apoptosis.[14] The contrasting effects of *Sox17* between humans and the mouse is somewhat surprising but could be partially attributed to the difference in expression during early hematopoiesis (see previous paragraph). The expression of all of the *SOXF* subfamily genes in ECs evokes the possibility that they have redundant function in the development of hematopoiesis from hESCs, as they do in postnatal angiogenesis in mice.[11] Nonetheless, the effects of knock-down of *Sox7* in mice and *SOX17* in the present study are different. *Sox7* knock-down in Brachyury+Flk1− mesodermal precursors, which give rise on further differentiation to Flk1+ cells containing hemangioblast precursors, profoundly inhibited the production of both hematopoietic progenitors and endothelial progenitors, leaving open the possibility that Sox7 inhibits the production of hematopoietic progenitors through inhibiting the formation of HE or hemangioblasts. In contrast, *SOX17* knock-down in ECs enriched in HE in the present study mainly compromised the development of mature hematopoietic cells and only mildly affected the proliferation of nonhematopoietic cells. Furthermore, depletion of *SOX17* in pre-HPCs did not significantly affect their hematopoietic differentiation. Therefore, the role of SOX17 at the developmental stage of blood specification could be more specific to the establishment of a hemogenic program in mesodermal or endothelial precursors compared with that of Sox7. Although we did not detect the effects of *SOX17* knock-down in pre-HPCs, recent studies have shown that Sox17 also plays an important role in the maintenance of fetal and neonatal HSCs, but not adult HSCs.[12] Sox17 has also been demonstrated to confer fetal HSC characteristics to adult hematopoietic progenitors.[13] SOX17 may again exert its critical function at a stage later than the pre-HPC stage, when pre-HPCs/HPCs differentiate into embryonic HSCs.

Very similar results have been demonstrated in the murine system with the transcription factor *HoxA3*. *HoxA3* is a gene uniquely expressed in the embryonic vasculature, but not in the yolk sac vasculature. HoxA3 restrains hematopoietic differentiation of the earliest endothelial progenitors and can induce reversion

of the earliest hematopoietic progenitors into CD41-negative endothelial cells.[29] This reversible modulation of endothelial-hematopoietic state is accomplished by down-regulation of key hematopoietic transcription factors. Among these, Runx1 is able to erase the endothelial program set up by *HoxA3* and promote hematopoietic differentiation. *Sox17* was listed as one of the targets regulated by HoxA3. Given that SOX17 appeared to regulate directly the expression of RUNX1 in this study, it could be assumed that HoxA3 functions as an apical regulator of HE, eventually activating the transcription of *Runx1* via up-regulation of *Sox17* to initiate hematopoietic differentiation. It would be intriguing to address this question.

The direct targets for Sox17 have been characterized during endodermal differentiation of mouse ESCs using ChIP-on-chip analysis. The Sox17-binding consensus motif has also been identified using de novo motif analysis from the ChIP-on-chip data.[22] As expected, the genes bound by Sox17 in *Sox17*-overexpressing HE-like cells were quite different from those detected during endodermal differentiation and were related to the GO terms "vasculogenesis," "hemopoiesis," or "positive regulation of erythrocyte differentiation." Among these genes, *VE-cadherin/CDH5* encodes one of the well-known marker antigens of HE and is also expressed by embryonic HSCs.[24,25] Sox17 appears to bind directly to the promoters of *RUNX1*, *SCL/TAL1*, and *HHEX*, which encode key transcription factors essential to the development of HSCs from HE cells or hemangioblasts.[4,26,27] Other target genes included *BAZF/BCL6B*, *JUNB*, and *EGFL7*, which encode a POZ/BTB zinc finger protein, a basic HLH transcription factor, and a secreted angiogenic factor, respectively. These genes have been implicated in vasculogenesis and/or angiogenesis and BAZF/BCL6B and JUNB have also been implicated in hematopoiesis.[30-34] The profiles of these Sox17 targets during early hematopoietic development further support the critical role of SOX17 in the regulation of HE.

The results of the present study have unveiled a novel function of SOX17 in hematopoietic development. Because the overexpression of *Sox17* expands HE-like cells, it is possible that conditional expression of *SOX17* in hESC-derived endothelial progenitors facilitates hematopoietic development. Therefore, *SOX17* could be a novel target for manipulation to improve the yield of hematopoietic progenies from hESCs for regenerative cell therapies.

Authorship

Contribution: Y. N.-T. performed the experiments, analyzed the results, produced the figures, and wrote the manuscript; M. Osawa,

References

1. Wang LD, Wagers AJ. Dynamic niches in the origination and differentiation of haematopoietic stem cells. *Nat Rev Mol Cell Biol.* 2011;12(10): 643-655.

2. Bertrand JY, Chi NC, Santoso B, Teng S, Stainier DY, Traver D. Haematopoietic stem cells derive directly from aortic endothelium during development. *Nature.* 2010;464(7285):108-111.

3. Boisset JC, van Cappellen W, Andrieu-Soler C, Galjart N, Dzierzak E, Robin C. In vivo imaging of haematopoietic cells emerging from the mouse aortic endothelium. *Nature.* 2010;464(7285):116-120.

4. Kissa K, Herbomel P. Blood stem cells emerge from aortic endothelium by a novel type of cell transition. *Nature.* 2010;464(7285):112-115.

5. Chen MJ, Yokomizo T, Zeigler BM, Dzierzak E, Speck NA. Runx1 is required for the endothelial to haematopoietic cell transition but not thereafter. *Nature.* 2009;457(7231):887-891.

6. North T, Gu TL, Stacy T, et al. Cbfa2 is required for the formation of intra-aortic hematopoietic clusters. *Development.* 1999;126(11):2563-2575.

7. North TE, de Bruijn MF, Stacy T, et al. Runx1 expression marks long-term repopulating hematopoietic stem cells in the midgestation mouse embryo. *Immunity.* 2002;16(5):661-672.

8. Lancrin C, Sroczynska P, Stephenson C, Allen T, Kouskoff V, Lacaud G. The haemangioblast generates haematopoietic cells through a haematogenic endothelium stage. *Nature.* 2009; 457(7231):892-895.

9. Kaufman DS. Toward clinical therapies using hematopoietic cells derived from human pluripotent stem cells. *Blood.* 2009;114(17):3513-3523.

10. Kanai-Azuma M, Kanai Y, Gad JM, et al. Depletion of definitive gut endoderm in Sox17-null mutant mice. *Development.* 2002;129(10):2367-2379.

11. Matsui T, Kanai-Azuma M, Hara K, et al. Redundant roles of Sox17 and Sox18 in postnatal angiogenesis in mice. *J Cell Sci.* 2006;119(Pt 17): 3513-3526.

12. Kim I, Saunders TL, Morrison SJ. Sox17 dependence distinguishes the transcriptional regulation of fetal from adult hematopoietic stem cells. *Cell.* 2007;130(3):470-483.

13. He S, Kim I, Lim MS, Morrison SJ. Sox17 expression confers self-renewal potential and fetal stem cell characteristics upon adult hematopoietic progenitors. *Genes Dev.* 2011;25(15):1613-1627.

14. Gandillet A, Serrano AG, Pearson S, Lie-A-Ling M, Lacaud G, Kouskoff V. Sox7-sustained expression alters the balance between proliferation and differentiation of hematopoietic progenitors at the onset of blood specification. *Blood.* 2009;114(23):4813-4822.

15. Serrano AG, Gandillet A, Pearson S, Lacaud G, Kouskoff V. Contrasting effects of Sox17- and Sox18-sustained expression at the onset of blood specification. *Blood.* 2010;115(19):3895-3898.

16. Ory DS, Neugeboren BA, Mulligan RC. A stable human-derived packaging cell line for production of high titer retrovirus/vesicular stomatitis virus G pseudotypes. *Proc Natl Acad Sci U S A.* 1996; 93(21):11400-11406.

17. Katayama K, Wada K, Miyoshi H, et al. RNA interfering approach for clarifying the PPARgamma pathway using lentiviral vector expressing short hairpin RNA. *FEBS Lett.* 2004;560(1-3):178-182.

18. Oshima M, Endoh M, Endo TA, et al. Genome-wide analysis of target genes regulated by HoxB4 in hematopoietic stem and progenitor cells developing from embryonic stem cells. *Blood.* 2011; 117(15):e142-150.

19. van Bakel H, van Werven FJ, Radonjic M, et al. Improved genome-wide localization by ChIP-chip using double-round T7 RNA polymerase-based amplification. *Nucleic Acids Res.* 2008;36(4):e21.

20. Vodyanik MA, Thomson JA, Slukvin II. Leukosialin (CD43) defines hematopoietic progenitors in human embryonic stem cell differentiation cultures. *Blood.* 2006;108(6):2095-2105.

21. Choi KD, Vodyanik M, Slukvin II. Hematopoietic differentiation and production of mature myeloid cells from human pluripotent stem cells. *Nat Protoc.* 2011;6(3):296-313.

22. Niakan KK, Ji H, Maehr R, et al. Sox17 promotes differentiation in mouse embryonic stem cells by directly regulating extraembryonic gene expression and indirectly antagonizing self-renewal. *Genes Dev.* 2010;24(3):312-326.

23. Nishikawa SI, Nishikawa S, Hirashima M, Matsuyoshi N, Kodama H. Progressive lineage analysis by cell sorting and culture identifies

FLK1+VE-cadherin+ cells at a diverging point of endothelial and hemopoietic lineages. *Development.* 1998;125(9):1747-1757.

24. Kim I, Yilmaz OH, Morrison SJ. CD144 (VE-cadherin) is transiently expressed by fetal liver hematopoietic stem cells. *Blood.* 2005;106(3): 903-905.

25. Taoudi S, Gonneau C, Moore K, et al. Extensive hematopoietic stem cell generation in the AGM region via maturation of VE-cadherin+CD45+ pre-definitive HSCs. *Cell Stem Cell.* 2008;3(1): 99-108.

26. Shivdasani RA, Mayer EL, Orkin SH. Absence of blood formation in mice lacking the T-cell leukaemia oncoprotein tal-1/SCL. *Nature.* 1995; 373(6513):432-434.

27. Guo Y, Chan R, Ramsey H, et al. The homeoprotein Hex is required for hemangioblast differentiation. *Blood.* 2003;102(7):2428-2435.

28. Costa G, Mazan A, Gandillet A, Pearson S, Lacaud G, Kouskoff V. SOX7 regulates the expression of VE-cadherin in the haemogenic endothelium at the onset of haematopoietic development. *Development.* 2012;139(9):1587-1598.

29. Iacovino M, Chong D, Szatmari I, et al. HoxA3 is an apical regulator of heamogenic endothelium. *Nat Cell Biol.* 2011;13(1):72-78.

30. Broxmeyer HE, Sehra S, Cooper S, et al. Aberrant regulation of hematopoiesis by T cells in BAZF-deficient mice. *Mol Cell Biol.* 2007;27(15): 5275-5285.

31. Ohnuki H, Inoue H, Takemori N, et al. BAZF, a novel component of cullin3-based E3 ligase complex, mediates VEGFR and Notch cross-signalling in angiogenesis. *Blood.* 2012;119(11): 2688-2698.

32. Licht AH, Pein OT, Florin L, et al. JunB is required for endothelial cell morphogenesis by regulating core-binding factor beta. *J Cell Biol.* 2006;175(6): 981-991.

33. Passegué E, Wagner EF, Weissman IL. JunB deficiency leads to a myeloproliferative disorder arising from hematopoietic stem cells. *Cell.* 2004; 119(3):431-443.

34. Nichol D, Stuhlmann H. EGFL7: a unique angiogenic signaling factor in vascular development and disease. *Blood.* 2012;119(6):1345-1352.

Development of an All-in-One Inducible Lentiviral Vector for Gene Specific Analysis of Reprogramming

Tomoyuki Yamaguchi[1,2]*, Sanae Hamanaka[1,2], Akihide Kamiya[2¤], Motohito Okabe[2], Mami Kawarai[1], Yukiko Wakiyama[1], Ayumi Umino[1], Tomonari Hayama[1,2], Hideyuki Sato[1], Youn-Su Lee[1,2], Megumi Kato-Itoh[1], Hideki Masaki[1,2], Toshihiro Kobayashi[1,2], Satoshi Yamazaki[1], Hiromitsu Nakauchi[1,2]*

1 Japan Science Technology Agency, ERATO, Nakauchi Stem Cell and Organ Regeneration Project, Tokyo, Japan, 2 Division of Stem Cell Therapy, Center for Stem Cell Biology and Regenerative Medicine, Institute of Medical Science, University of Tokyo, Tokyo, Japan

Abstract

Fair comparison of reprogramming efficiencies and *in vitro* differentiation capabilities among induced pluripotent stem cell (iPSC) lines has been hampered by the cellular and genetic heterogeneity of de novo infected somatic cells. In order to address this problem, we constructed a single cassette all-in-one inducible lentiviral vector (Ai-LV) for the expression of three reprogramming factors (*Oct3/4, Klf4* and *Sox2*). To obtain multiple types of somatic cells having the same genetic background, we generated reprogrammable chimeric mice using iPSCs derived from Ai-LV infected somatic cells. Then, hepatic cells, hematopoietic cells and fibroblasts were isolated at different developmental stages from the chimeric mice, and reprogrammed again to generate 2nd iPSCs. The results revealed that somatic cells, especially fetal hepatoblasts were reprogrammed 1200 times more efficiently than adult hepatocytes with maximum reprogramming efficiency reaching 12.5%. However, we found that forced expression of *c-Myc* compensated for the reduced reprogramming efficiency in aged somatic cells without affecting cell proliferation. All these findings suggest that the Ai-LV system enables us to generate a panel of iPSC clones derived from various tissues with the same genetic background, and thus provides an invaluable tool for iPSC research.

Introduction

Induced pluripotent stem cells (iPSCs) are artificial pluripotent stem cells originally generated from mouse somatic cells in 2006 [1] and from human somatic in 2007 [2,3] by the enforced expression of four transcription factors (*Oct 4, Sox2, c-Myc,* and *Klf4*); genes that are expressed in embryonic stem cells (ESCs). IPSCs are alkaline phosphatase positive and morphologically similar to ESCs and are likewise capable of differentiating into cell types representative of all three germ layers: ectoderm, endoderm, and mesoderm. Moreover, gene expression profiles, chromatin methylation patterns and doubling time of iPSCs closely resemble those of ESCs, but the full extent of their relationship is still being evaluated. Besides the ethical issues surrounding the use of human embryos, there is a technical problem of graft-versus-host disease associated with allogeneic stem cell transplantation. However, these problems may be solved using autologous iPSCs and this is an important advantage of iPSCs relative to ESCs in the development of iPSCs-based therapies. On the other hand, detailed mechanisms of reprogramming or differentiation capacity of iPSCs are not clearly understood and elucidation of these subjects is important to both basic and translational research. A number of methods for generating iPSCs have been reported. These include DNA [4,5,6,7], RNA [8,9] and protein [10]

transfection as well as the viral delivery systems including retrovirus [1], lentivirus [11,12], adenovirus [13] and sendaivirus [14,15]. Because iPSCs are generally produced by the over-expression of three or four transcriptional factors, the generated clones display genetic heterogeneity and this is an obstacle to understanding their mechanisms of reprogramming and phenotypes. In light of this problem, several groups have reported a reprogrammable mouse system using transgenic mice carrying two tetracycline (tet) inducible vectors consisting of a tet responsive element (TRE) driven TA peptide connected to four reprogramming factors (*Oct3/4, Klf4, Sox2* and *c-Myc*) and reverse tet transactivator (rtTA) on the ROSA locus [11,12,16,17]. Because somatic cells isolated from reprogrammable mice or their iPSCs carry the same genetic background, a fair comparison of reprogramming efficiency or phenotype of iPSCs are possible.

One of the proto-oncogenes, *Myc* is known to interact with proteins essential for transcriptional regulation such as transformation/transcription domain-associated protein (TRRAP) or histone acetyltransferases (HAT), and this is considered to be important for multiple functions of *Myc*, like regulation of cell cycle, metabolism, differentiation, transformation and apoptosis [18,19]. *Myc* also plays a crucial role in reprogramming, since its absence significantly lowered reprogramming efficiency [20]. It has also been reported that the efficiency of germline transmission

— 190 —

of iPSCs largely depends on *Myc* transgenes [21,22]. However, these results were obtained using materials that were not genetically identical.

To circumvent this problem, we constructed a single cassette all-in-one inducible lentiviral vector (Ai-LV) for expression of three reprogramming genes (*Oct4*, *Sox2* and *Klf4*) self-cleaving 2A peptides and a tetracycline inducible expression module. It should be noted that somatic cells of different types are available from reprogrammable chimeric mice using iPSCs derived from Ai-LV infected somatic cells and the function of *c-Myc* on reprogramming can be easily analyzed by the additional expression of *c-Myc*. Moreover, because we used a single cassette, this system could easily create reprogrammable animals other than mouse; which could not be accomplished with the previous system.

Results

Generation of Primary iPSCs by All-in-one Inducible Lentiviral Vector (Ai-LV)

In order to generate a reprogrammable mouse strain, we constructed a Doxycyclin (Dox) dependent inducible lentiviral vector; encoding for tet-responsive element (TRE) regulation of murine versions of three reprogramming factors (Oct4, Klf4 and Sox2) and human ubiquitin C (ubc) promoter-driven reverse tet-transactivator (rtTA) and Enhanced Green Fluorescent Protein (EGFP) connected by an internal ribosomal entry site (IRES) (Fig. 1A). Under the control of a Ubc promoter, rtTA ubiquitously expressed in mouse tissues where it binds to TRE in the presence of Dox and initiates transcription of reprogramming factors. Ai-LV induced iPSCs can be used to generate chimeric mice, from which genetically identical tissues (e.g., fibroblast, hematopoietic cells and hepatic cells) can be isolated at different developmental stages. These tissues can be re-reprogrammed into iPSCs by the addition of Dox in the culture medium for analysis of their reprogramming potential. Moreover, it is possible to measure the differentiation capacity of the re-reprogrammed iPSCs *in vitro*. To further analyze the function of *Myc* during reprogramming, iPSCs generated by Ai-LV were infected with an additional inducible vector carrying myc for re-reprogramming, as described in Fig. 1A.

To generate reprogrammable chimeric mice, we infected mouse embryonic fibroblasts with Ai-LV and cultured with Dox-containing medium. Morphologically ES-like colonies appeared after six to eight days of infection, expressed EGFP and were of typical dome shape. Alkaline phosphatase (AP) staining revealed that all colonies were pluripotent and the number of AP$^+$ colonies were 51 at a multiplicity of infection (m.o.i.) of 0.4, 127 at 0.8 and 209 at 1.6, and the efficiency of reprogramming was 0.14% (Fig. 1B). On the other hand, no colonies appeared in Ai-LV infected cells cultured without Dox. Several iPS colonies were isolated and examined for the expression profiles of pluripotent marker genes including *c-Myc*, *Nanog*, *Rex*, *Gdf3*, *Eras*, *Zfp296*, *Ecat*, endogenous *Oct4*, endogenous *Klf4* and endogenous *Sox2* by RT-PCR. To detect transgene expression, we designed the primer to amplify the sequence between the T2A and *Klf4* sequence. As shown in Figure 1C, the pluripotent marker genes were expressed at quantities comparable to those in C57Bl/6 mouse ES cells (B6 ES) and the expression of transgene was detected only in Dox-treated iPSCs. This indicates that iPSCs generated by Ai-LV were completely reprogrammed and the expression from the lentiviral vector was tightly controlled by a TRE. Pluripotency of iPSCs was further confirmed by continuous expression of *Nanog* in both cases with or without Dox (Fig. 1D). To ask whether these clones are capable of re-reprogramming by adding Dox, we performed re-reprogramming of *in vitro* differentiated iPS clones (removal of

MEF and Lif for two weeks) and revealed re-reprogramming of all clones (Fig. S1A).

Southern blot analysis revealed that proviral copy numbers are one or two, indicating that one copy of Ai-LV is enough for induction of iPSCs (Fig. S1B).

These results indicate that iPSCs generated by Ai-LV were reprogrammed into a pluripotent state and transgene expression was tightly controlled by a tetracycline inducible expression module. Moreover the pluripotent states of iPSCs generated by Ai-LV were kept, regardless of transgene expression. Because the iPSCs#6 clone carries only one proviral copy and exhibits the highest levels of transgene expression among the four clones, this particular clone was chosen for the generation of chimeric mice. Before attempting to generate chimeric mice, we evaluated iPSCs #6 clone karyotypes; they were normal (40XY; Fig. S1C).

We also tried to generate human iPSCs (hiPSCs) by infection of 3×10^4 human neonatal dermal fibroblasts with Ai-LV encoding human version of three reprogramming factors (Oct4, Klf4 and Sox2) with or without human *c-MYC* encoding lentiviral vector; however we could only generate two hiPSC colonies when the *c-Myc* vector was infected. Then, we performed *in vitro* differentiation of hiPSCs and observed only iPS colonies in Dox-containing culture (Fig. S1D), indicating that the inducible system described here also works in human somatic cells.

Phenotype of Secondary iPSCs (2nd miPSCs)

Previous reports showed that iPSCs derived from murine tissues possessed residual DNA methylation signatures characteristic of their somatic tissue of origin, which tends to differentiate to lineages of the donor cell [23,24,25]. To analyze whether the miPSCs re-reprogrammed from chimeric mice (2nd miPSCs) posses this phenotype, we generated 2nd miPSCs from E13.5 fetal liver CD45$^+$ hematopoietic cells (FL CD45), adult dermal fibroblasts (Adult fb), adult hepatocytes (Adult hep) and E13.5 fetal hepatoblasts (Fetal hep) and compared their efficiency of induction to hematopoietic cells by *in vitro* differentiation assay (Fig. 2A). As shown in Fig. 2B, differentiation efficiency of each tissue type to CD41$^+$c-kit$^+$ primitive hematopoietic progenitor cells (primitive HPC) was 7.3%(FL CD45), 2.1% (Adult fb), 3.7% (Adult hep) and 2.0% (Fetal hep). Although no significant differences were observed in the efficiency of differentiation from CD41$^+$c-kit$^+$ primitive HPC to CD45+ hematopoietic cells (14.2%, 14.4%, 13.3% and 14.9%, respectively) after 4-day culture on OP9 stromal cells, overall differentiation capacity of 2nd miPSCs derived from FL CD45 to CD45$^+$ hematopoietic cells was over 2 folds higher than iPSCs derived from other tissues with a statistically significant difference (Fig. 2B). These results observed for our system coincide with previously described epigenetic memories in the 2nd miPSCs [25].

Analysis of Reprogramming Efficiency

We isolated fibroblasts, hematopoietic cells and hepatic cells from chimeric mice at different developmental stages (E13.5, newborn, one-week old and adult (four weeks old)), and re-reprogrammed these to generate 2nd miPSCs. Generated iPS colonies were stained with anti-nanog antibody at two weeks after Dox addition and nanog positive colonies were counted and reprogramming efficiency was calculated by dividing the total number of Nanog positive colonies by the number of seeded cells. The reprogramming efficiency of E13.5 fibroblast (MEF), newborn fibroblast (NB fb), one-week old fibroblast (1wk fb) and adult fibroblast (Adult fb) were 5.07%, 3.07%, 1.43% and 0.03%, respectively (Fig. 3B). These results indicate that reprogramming efficiency decreased as developmental stage progressed.
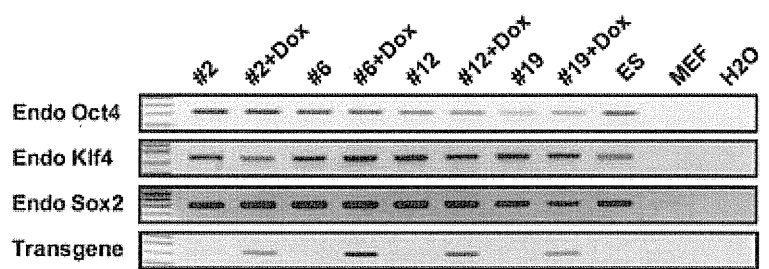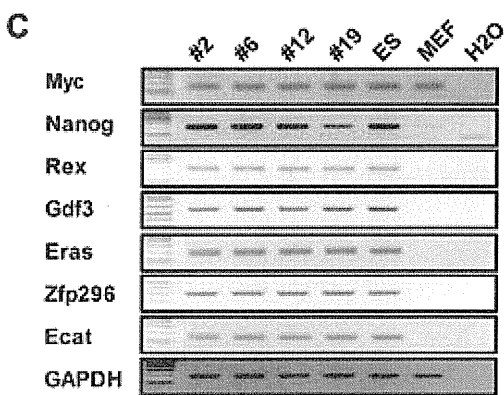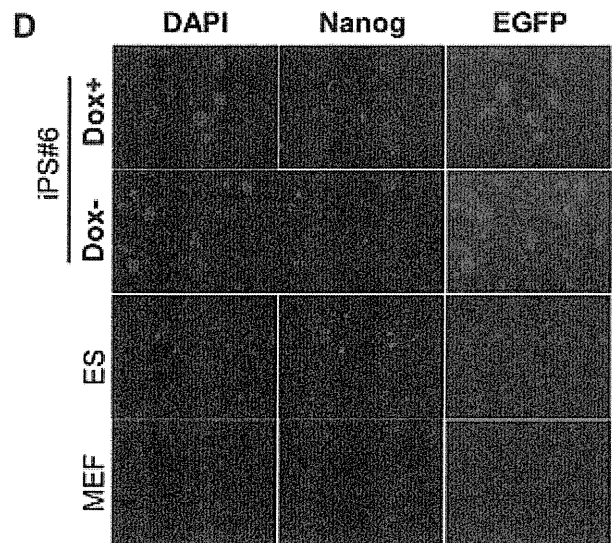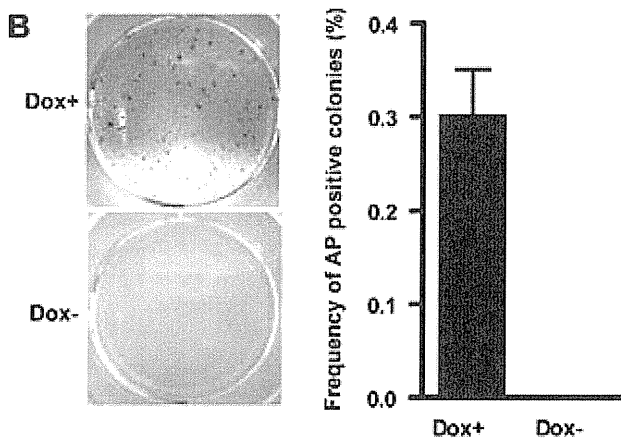
— 191 —
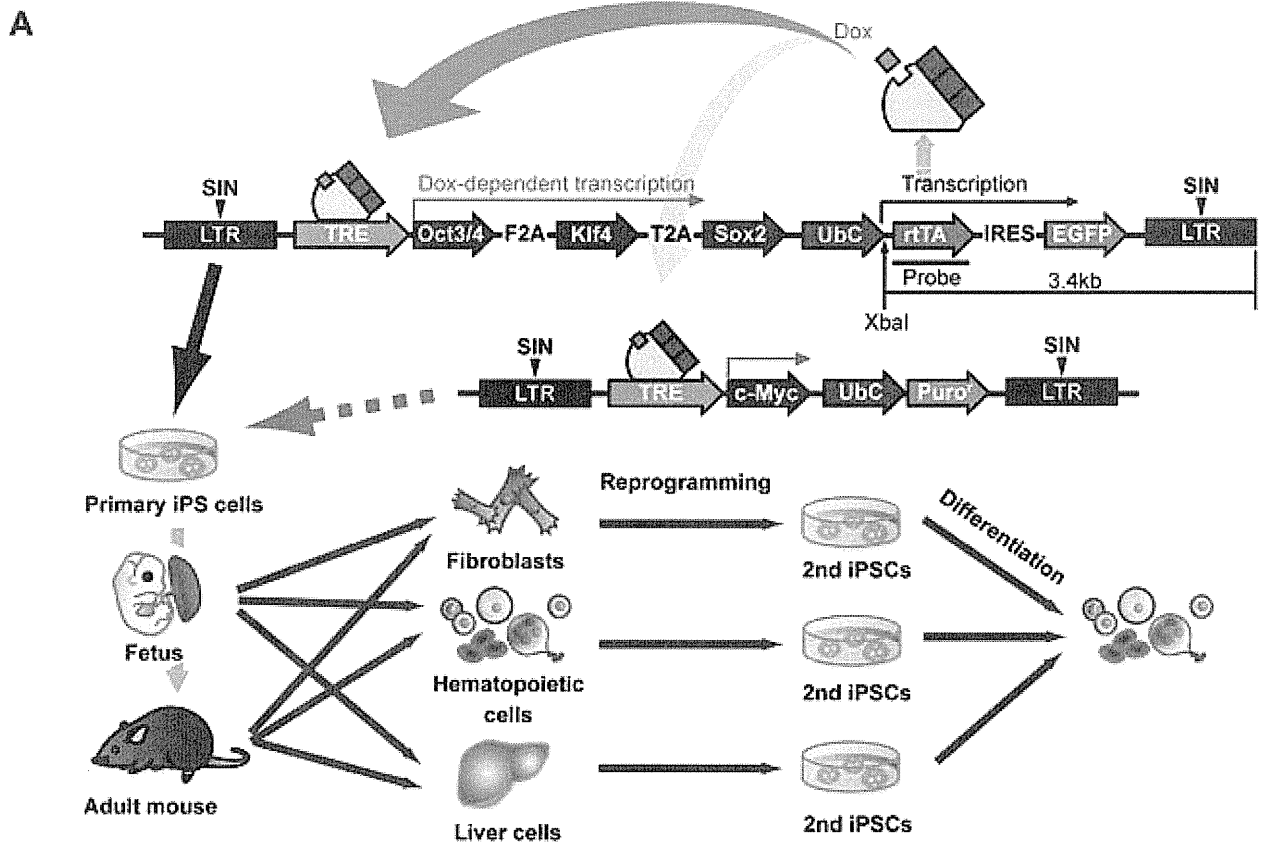
A

B

C

D

— 192 —

Figure 1. Construction of Dox inducible reprogramming system. (A) Schematic diagram of Dox inducible system for expression of reprogramming factors. (B) Alkaline phosphatase (AP) staining of iPS colonies derived from Ai-LV transduced MEFs (left panel). Efficiency of AP positive colonies (right panel). Efficiency of AP positive colonies calculated by dividing infected cell number by the number of AP positive colonies. (B) RT-PCR analysis of endogenous pluripotent marker genes, with or without Dox in the culture. (C) Immunofluorescence staining for *Nanog* in iPS clone#6, with or without Dox in the culture.
doi:10.1371/journal.pone.0041007.g001

Similar results were observed in reprogramming of hematopoietic cells. Only a few colonies were generated from adult hematopoietic cells; hematopoietic stem cells (HSC), hematopoietic progenitor cells (HPC), myeloid progenitor cells (MP) and macrophages (Mac), when compared with E13.5 CD45+ fetal liver hematopoietic cells (FL CD45) (efficiency was 1.47%) (Fig. 3B). The most remarkable difference was observed in hepatic cells. Fetal liver cells (Fetal hep) were 1200 times more efficiently reprogrammed than adult liver cells (Adult hep) (Fig. 3B). To elucidate whether this difference is attributable to cell division rate, we analyzed the proliferation of fibroblast (MEF, NB fb, 1wk fb and Adult fb) at three, four and five days after seeding with or without Dox. Doubling times were 9.5 hrs, 11.5 hrs, 12.6 hrs and 10.7 hrs, respectively in the absence of Dox; and 27.0 hrs, 21.0 hrs, 29.6 hrs and 25.6 hrs, respectively in the presence of Dox. Although slower proliferation was observed in Dox additive culture, statically no significant differences were observed among MEF, NB FB, 1wk FB and Adult FB (Fig. 3C). Furthermore, we compared the expression levels of reprogramming factors (*Oct4*, *Klf4*, *Sox2* and *c-Myc*) and senescence-related genes (*p19^{Arf}*, *p16^{INK4a}*, *p53* and *p21^{CIP1}*) in four fibroblasts cultured in the absence of Dox by RT-PCR. However, there were no significant differences in the expression of the reprogramming factors (Fig.

S2A) nor in the age dependent increase in senescence-related genes (Fig. S2B).

These results indicate that aging effects other than cell proliferation or expression levels of reprogramming factors or senescence-related genes reduced the reprogramming efficiency.

Effect of c-Myc Expression on Reprogramming

Previous report showed that four transcription factors (*Oct4*, *Klf4*, *Sox2* and *c-Myc*) can reprogram somatic tissues to pluripotency more efficiently than three factors (*Oct4*,*Klf4* and *Sox2*) [20]. Therefore, to ascertain whether this phenomenon is also observed in our system, we generated chimeric mice by transduction of a c-myc-encoded lentiviral vector into clone #6 (#6M). Then, somatic tissues from the chimeric mice were isolated and each reprogramming efficiency was determined. The efficiencies of four-factor reprogramming were 13.1% for MEF, 14.3% for NB fb, 13.4% for 1wk fb and 1.0% for Adult fb (Fig. 4A). Although the efficiencies of three-factor reprogramming declined as developmental stages progressed, we did not detect any significant differences among MEF, NB fb or 1wk fb by four-factor reprogramming (Fig. 4A). Similarly, the age-dependent decline of reprogramming in hematopoietic cells (FL CD45, HPC and MPC) was improved by *c-Myc* (Fig. 4A). Although lowered
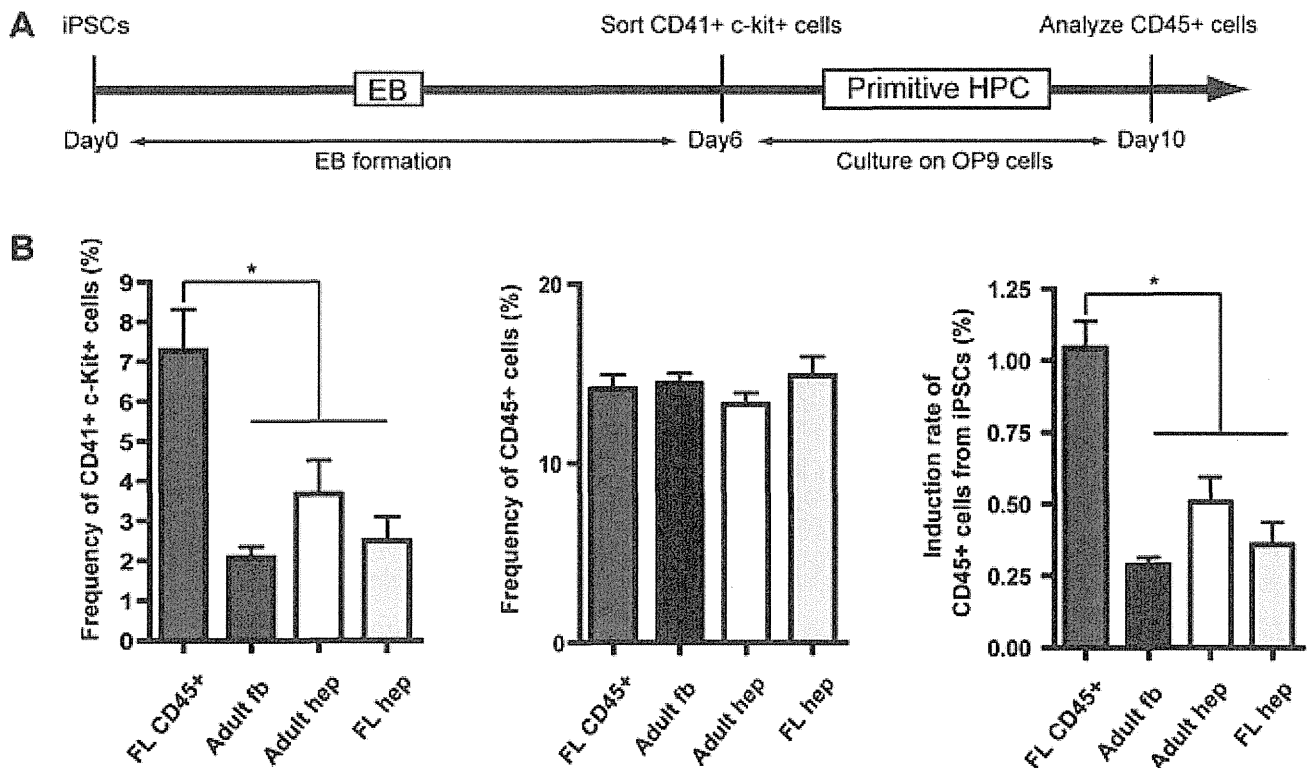

Figure 2. Differentiation capacity of iPSCs to hematopoietic cells. (A) Protocol for in vitro differentiation of iPSCs to hematopoietic cells. (B) Frequency of CD41+, c-Kit+ primitive hematopoietic progenitor in dissociated EB cells at day six. *p<0.05 (left). Frequency of CD45+ hematopoietic cells in sorted CD41+, c-Kit+ cells cultured on OP9 feeder layer for four days (middle). Total induction rate of CD45+ hematopoietic cells from iPSCs were analyzed. *p<0.05 (right).
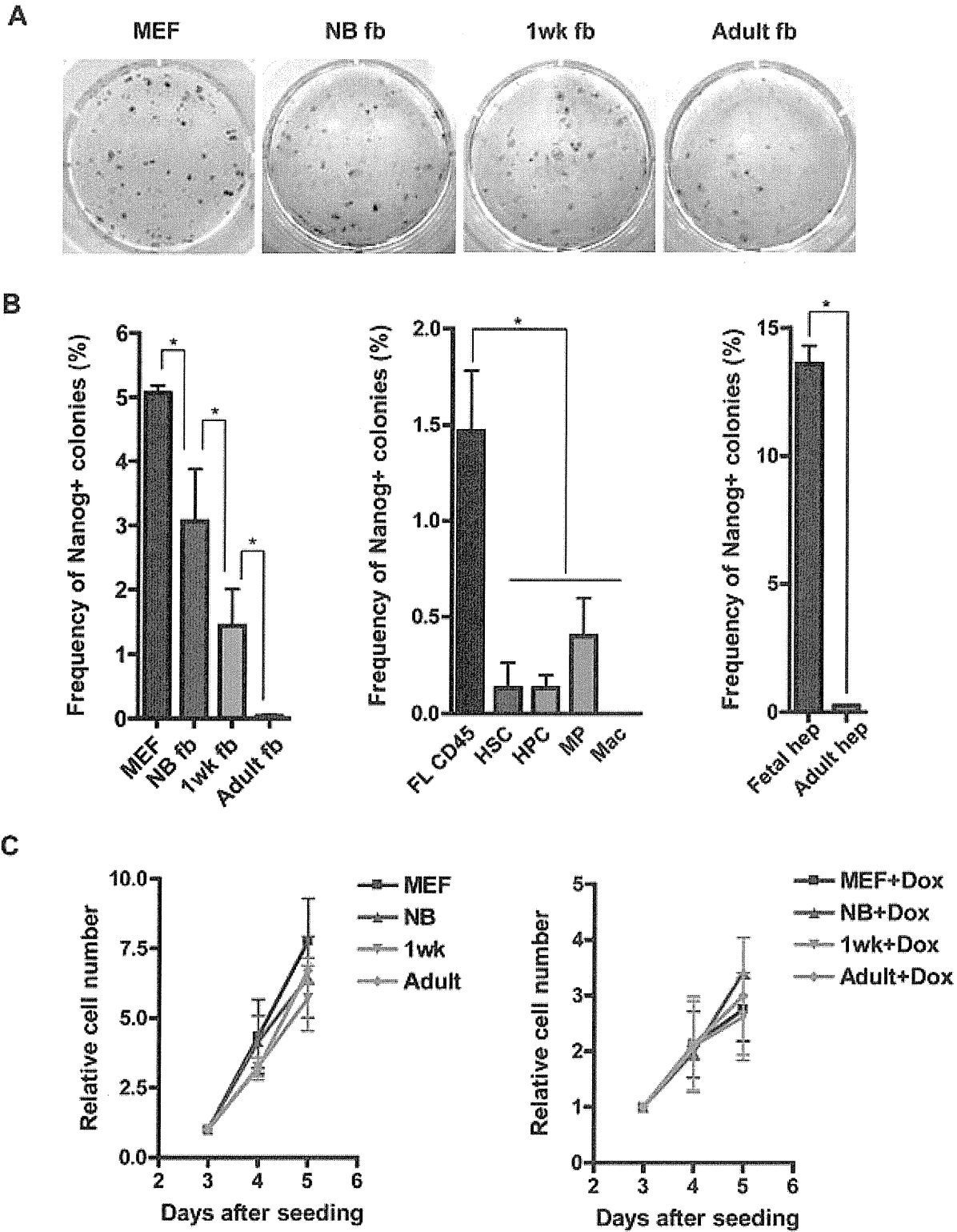doi:10.1371/journal.pone.0041007.g002

— 193 —

Figure 3. Reprogramming efficiency from somatic cells at different developmental stages. (A) *Nanog* immunostaining of 2nd iPS colonies derived from MEF (2000 cells), NB fb (2000 cells), 1wk fb (5000 cells) and Adult fb (10000 cells). Each cell were seeded on a feeder layer and cultured in the presence of Dox for two weeks. (B) Reprogramming efficiency of fibroblasts (MEF, NB fb, 1wk fb and Adult fb) *p<0.05 (left panel), hematopoietic cells (FL CD45, HSC, HPC, MP and Mac) *p<0.05 (middle panel) and liver cells (Fetal hep and Adult hep) *p<0.01 (right panel) were analyzed by dividing seeded cell number by the number of *Nanog* positive colonies. (C) Cell proliferation rate of fibroblasts (MEF, NB fb, 1wk fb and Adult fb) at three, four and five days after seeded in the absence of Dox (left) and in the presence of Dox (right).
doi:10.1371/journal.pone.0041007.g003

—194—

reprogramming efficiency (0.53%) was observed in HSC culture at two weeks after Dox addition, the efficiency reached to 22.6% at three weeks, without any significant difference between HPC (34%) (data not shown). Given the oncogenic properties of c-Myc, we analyzed the cell proliferation rate of fibroblasts as described above and observed that there are statically no significant differences among fibroblasts isolated from the four-factor chimeric mice (Fig. 4B). Because the previous study showed that histone deacetylase inhibitor, valproic acid (VPA) [26,27], can substitute for Myc in iPSCs generation, we analyzed whether VPA can substitute for Myc in our system. However, VPA did not increase the reprogramming efficiency in our system (Fig. 4C). These results indicate that c-Myc can cancel the aging effects on reprogramming efficiency in some types of cells and reprogramming recovery by c-Myc is not necessarily related to histone acetylation.

Reprogramming Efficiency of Somatic Tissues from other Species

We previously reported the successful generation of reprogrammable rat by Ai-LV, and one of the features of our vector system is that it is not limited to an inducible mouse model [28,29]. By using this reprogrammable rat, we compared the reprogramming efficiency of rat fibroblasts (embryonic fibroblasts (REF), one-week fibroblasts (r1wk fb) and adult fibroblast (rAdult fb)) at 3weeks after seeding. Reprogramming efficiency of REF, r1wk fb and rAdult fb were 0.9%, 0% and 0%, respectively (Fig. 5A). We also analyzed the proliferation of REF, r1wk fb and rAdult fb at six, nine and twelve days after seeding in the presence of Dox and we found that statically no significant differences were observed (Fig. 5B).

These results indicate that the aging-dependent decline of reprogramming efficiency is also seen in rat somatic cells and this is independent of cell proliferation rate. To analyze c-Myc functions to initiate reprogramming, we infected REF, r1wk fb and rAdult fb with inducible a lentiviral vector carrying the c-Myc gene. The reprogramming efficiencies of these tissues were 0.9%, 1.0% and 1.2%, respectively, indicating that expression of c-Myc in addition to Oct4, Sox2 and Klf4 can cancel the aging effects as seen in mouse somatic cells (Fig. 5A).

Discussion

We here document a novel vector system which allows Dox-inducible gene expression of 2A linked three reprogramming factors. Unlike the previous system, iPSCs can be induced by a single vector carrying both TRE and rtTA cassettes. In the previous report, only a small percentage of MEF (approximately 0.0084%) was reprogrammed with both the Dox inducible lentiviral vector carrying 2A linked four reprogramming factors (Oct4, Klf4, Sox2 and c-Myc) and the rtTA vector [12]. On the other hand, in spite of using only three factors, the reprogramming efficiency from Ai-LV infection was approximately twenty times higher than the previous system. This is one of the benefits of a single cassette Ai-LV system. Moreover, it can be more easily constructed with a variety of species. On the other hand, in contrast to previous report we could not generate hiPSCs by Ai-LV in the absence of hc-MYC [20]. The possible explanations for this result can be follows; #1; we may require over 5×10^4 cells for infection. #2; the expression condition for reprogramming factors from Ai-LV may not be optimal [30].

Although we could not generate F1 mice from iPS#6, a certain degree of germ cell contribution was observed in chimeric mice (data not shown). A previous report showed that immature histone

acetylation by three reprogramming factors leads to lower efficiency of germline transmission as compared to four reprogramming factors [22]. Since the lowered efficiency was recovered by histone deacetylase inhibitor Tricostatin A (TSA), it is possible to generate F1 mice from iPS#6 by the same treatment. Moreover, because our previous study showed that rat iPSCs derived from Ai-LV infected REF can generate an F1 rat, Ai-LV is considered to have the potential to generate germline competent pluripotent stem cells [28].

As previously described, we found that 2nd iPSCs generated by our reprogramming system posses the functional properties of the original cell type which influences the directed differentiation of iPSCs to their tissue of origin [23,24,25]. It should be noted that iPSCs generated by our three factors system exhibit the same profiles as those generated by four factors, including c-Myc, suggesting that the epigenetic memory of iPSCs is retained regardless of c-Myc status.

There are two major findings in the present study. First, reprogramming efficiency by three factors tends to decrease as developmental stage progressed in several kinds of somatic tissues including fibroblast, hematopoietic cells and hepatic cells. It has been previously reported that up-regulation of senescent effectors $p16^{INK4a}$, $p53$ and $p21^{CIP1}$ impairs successful reprogramming [31]. However, we could not detect aging related up-regulation of those effectors among the four kinds of fibroblasts. Moreover, with respect to cell growth, there was no significant difference between embryonic cells (MEF, FL CD45) and aged tissues (NB fb, 1wk fb, Adult fb, HSC, HPC, and MP). Likewise, aged cells did not display characteristic senescence morphology until the iPS colonies started to appear in the embryonic cell culture; indicating that the aging effect other than induction of senescence reduces the efficiency of reprogramming.

Second, addition of c-Myc to three factors improved the age related decreases in reprogramming efficiency of mouse and rat somatic cells (NB fb, 1wk fb, r1wk fb, rAdult fb, HSC, HPC, and MP). It has been reported that myc increases reprogramming efficiency via chromatin remodeling by recruiting histone acetylase or histone/DNA demethylase [22,32]. Although histone deacetylase inhibitor VPA could not substitute for c-Myc in our system, it is still possible that c-Myc may be involved in improving the age related decrease in reprogramming efficiency through histone/DNA demethylation. Moreover, previous reports showed that increased expression of TERT, a catalytic subunit of telomerase is important for reprogramming by maintaining telomere length [33]. On the other hand, in spite of c-Myc overexpression, decreased reprogramming efficiency did not recover in Adult fb, mac or Adult hep. These results are similar to previously reported four factors reprogramming systems and may be due to inhibitory mechanisms for which c-Myc cannot compensate. For instance, higher expression of the ATP-dependent BAF chromatin-remodeling complex in fetal liver cells compared to adult liver cells leads to higher reprogramming efficiency and this is independent of c-Myc expression [34]. Thus, various factors appear to be associated with age-related decrease in reprogramming and our system is valuable for exploration of those factors.

In conclusion, our Ai-LV system revealed the link between aging and reprogramming efficiency and will help us to understand the detailed molecular mechanisms of reprogramming.

Materials and Methods

Lentiviral Vector Construction and Preparation

All-in-one inducible lentiviral vector (Ai-LV) was derived from the self-inactivating (SIN) lentiviral vector CS-CDF-CG-PRE [35].
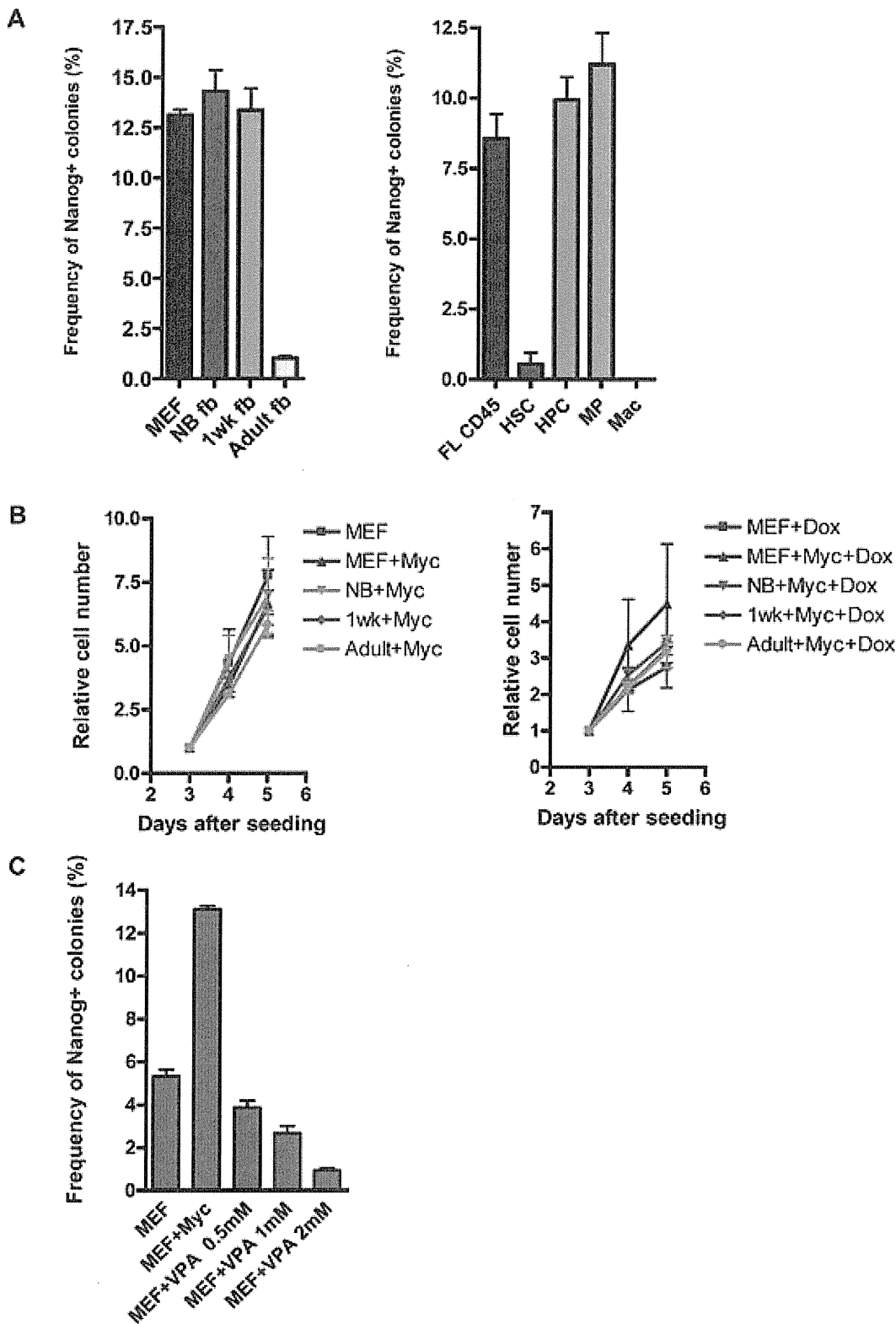
— 195 —

Figure 4. Reprogramming efficiency of somatic cells in the presence of c-Myc. (A) Reprogramming efficiency of fibroblasts (MEF, NB fb, 1wk fb and Adult fb), hematopoietic cells (FL CD45, HSC, HPC, MP and Mac) by four reprogramming factors including c-Myc. (B) Cell proliferation rate of fibroblasts (MEF, NB fb, 1wk fb and Adult fb) at three, four and five days after seeded in the absence of Dox (left) and in the presence of Dox (right). (C) Reprogramming efficiency of MEF were compared between reprogrammed by three factors (Oct4, Klf4 and Sox2), four factors (Oct4, Klf4, Sox2 and c-Myc) and three factors plus VPA (0.5 mM, 1 mM and 2 mM).
doi:10.1371/journal.pone.0041007.g004
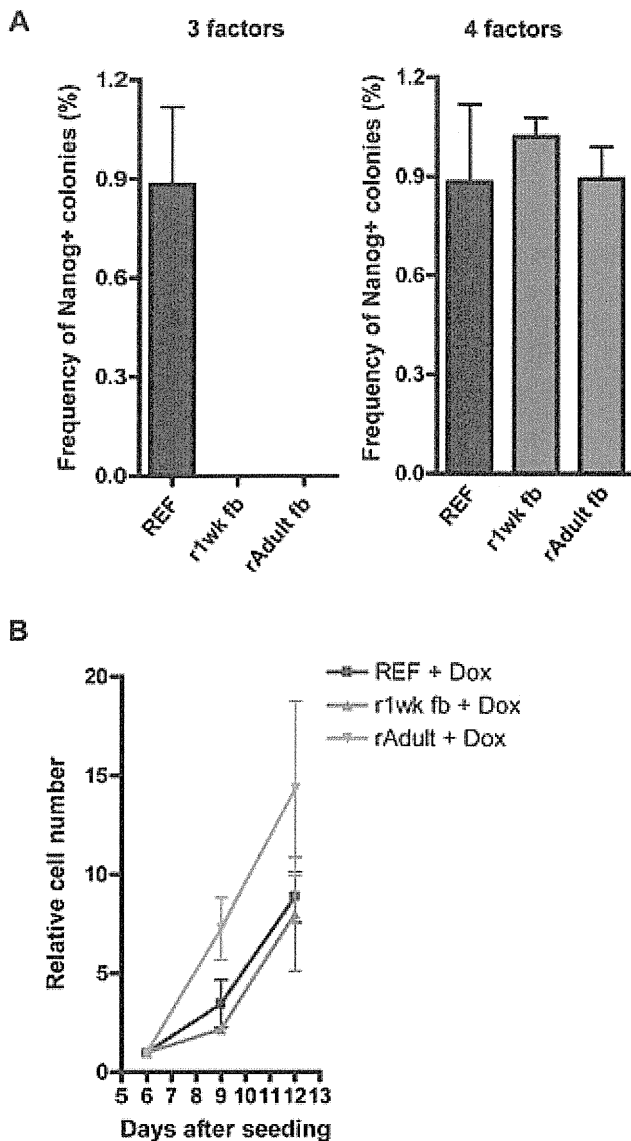
A

3 factors   **4 factors**

B

Figure 5. Reprogramming efficiency of rat somatic cells. (A) Reprogramming efficiency of rat fibroblasts (REF, r1wk fb and rAdult fb) by three reprogramming factors (*Oct4, Klf4* and *Sox2*) (left) and by four reprogramming factors (*Oct4, Klf4, Sox2* and *c-Myc*) (right). (B) Cell proliferation rate of rat fibroblasts in the presence of Dox.
doi:10.1371/journal.pone.0041007.g005

Mouse *Oct4, Sox2* and *Klf4* linked by the 2A sequence (BsiWI-EcoRI) was cloned into T7 blue cloning vector (Takara Bio, Shiga, Japan) resulting in T7 mOKS. Polymerase chain reaction (PCR)-amplified TRE fragment (MfeI- BsiWI, EcoRI, NheI, XbaI and XhoI) from pTRE-tight (Clontech Inc. California, USA) was cloned into the EcoRI-XhoI site of CS-CDF-CG-PRE resulting CS-TRE-PRE. PCR-amplified PRE (EcoRI-NheI), human Ubiquitin C (Ubc) promoter (NheI-XbaI), reverse tet tarnsactivator (rtTA) (XbaI-XhoI) from pTet-on Advanced (CLONTECH) and IRES2 EGFP (XhoI-XhoI) from pIRES2-EGFP were cloned into the EcoRI-NheI site, NheI-XbaI site, XbaI-XhoI site and XhoI site of CS-TRE-PRE, respectively, resulting in CS-TRE-PRE-Ubc-tTA-I2G. Then a BsiWI-EcoRI fragment of T7 mOKS was inserted into BsiWI-EcoRI sites of CS-TRE-PRE-Ubc-tTA-I2G resulting in CS-TRE-mOKS-PRE-Ubc-tTA-I2G. For *c-Myc*

expression, PCR-amplified *c-Myc* (BsiWI-EcoRI) and Puromycin resistant gene (XbaI-XhoI) were cloned into CS-TRE-mOKS-PRE-Ubc-tTA-I2G resulting in CS-TRE-c-Myc-Ubc-puro. Lentiviral vectors pseudotyped with the vesicular stomatitis virus G glycoprotein were produced as described previously.

Cell Culture

Mouse embryonic fibroblasts (MEFs) were cultured in Dulbecco's modified Eagle's medium (DMEM; Sigma, St. Louis, MO) supplemented with 10% fetal bovine serum (FBS; Hana-Nesco Bio, Moregate BioTech, Australia), 1% L-glutamine penicillin streptomycin (Sigma, St. Louis, MO). Mouse iPS cells (miPSCs) were maintained on mitomycin-c treated mouse embryonic fibroblasts (MEFs) in ES/iPS medium: DMEM supplemented with 15% fetal bovine serum (FBS; Nichirei Bioscience, Tokyo, Japan), 0.1 mM 2-mercaptoethanol (Invitrogen, San Diego, CA, USA), 0.1 mM nonessential amino acids (Invitrogen), 1 mM sodium pyruvate (Invitrogen), 1% L-glutamine penicillin streptomycin (Sigma), and 1000 U/ml of mouse leukemia inhibitory factor (LIF; Millipore, Bedford, MA, USA). Rat iPS cells (riPSCs) were maintained as previously described.

In vitro Differentiation of miPSCs

To allow miPSCs to differentiate into EBs, iPSCs were trypsinized and collected in complete EB differentiation medium (EBD) [36]. Cells were transferred into a 100-mm Petri dish at 2×10^5 cells per 10 ml EBD. The medium was changed on day four of culture and every two days thereafter. On day six, EBs were trypsinized and stained with phycoerythrin-conjugated (PE-) anti-mouse CD41 and allophycocyanin-conjugated (APC-) anti-mouse c-Kit antibodies (BD Biosciences, San Jose, CA) and sorted $CD41^+, c-Kit^+$ cells on OP9 cells. OP9 cells were maintained in α-MEM containing 15% FCS. 10^5 OP9 cells were plated in each well of a 6-well tissue culture plate two days before starting co-culture. Co-cultures were employed with IMDM containing 20 ng/ml mouse stem cell factor (SCF) and 20 ng/ml human thrombopoietin (TPO) (PeproTech, Rocky Hill, NJ), 10% FCS, 2 mM L-Gln, 0.1 mM 2-ME, and 100 U/ml penicillin/streptomycin. On day four of co-culture, cells were recovered from the culture dishes for analysis on a flow cytometer.

Generation of Primary iPSCs and Chimeric Mice

To establish miPSCs MEFs were transduced with Ai-LV and cultured in the presence of Dox (2 ug/ml). Eight days later, generated colonies were picked up and mechanically dissociated cells were placed on MEFs feeder. Chimeric mice were generated by injection of primary miPSCs into day 4.5 blastocysts of ICR female mice, followed by transfer into host uteri as previously described [29]. All of the studies were derived from independent founder animals.

Isolation of Somatic Cells

Mouse and rat fibroblasts including MEF, REF, NB fb, 1wk fb, r1wk fb, Adult fb and rAdult fb were isolated from E13.5 mouse embryo, E14.5 rat embryo, new born mice, one-week-old mice, one-week-old rats, four-week-old mice and four-week-old rats, respectively. GFP+ mouse fibroblasts were sorted on a feeder layer by a MoFlo™ flow cytometer. For isolation of FL CD45+ cells, E13.5 fetal liver cells were stained with allophycocyanin (APC)-conjugated anti-mouse CD45 (BD Biosciences) and sorted on a feeder layer by a MoFlo™ flow cytometer. For isolation of Hematopoietic stem cells (HSCs) $(CD34^-, c-Kit^+, Sca1^+, lin^-)$, Hematopoietic progenitor cells (HPCs) $(CD34^+, c-Kit^+, Sca1^+,$-

— 197 —

lin$^-$) and Myeloid progenitor (MP) (c-Kit$^+$, Sca1$^-$, lin$^-$), Bone marrow (BM)cells from four-week-old mice were stained with an antibody mixture consisting of anti-mouse biotinylated anti-Gr-1, anti-Mac-1, anti-CD45R, anti-CD4, anti-CD8, anti-IL-7R, and anti-TER119 antibodies (eBioscience). Lineage$^+$ cells were then depleted using MACS anti-biotin microbeads and a LS-MACS system (Miltenyi Biotec, Bergisch Gladbach, Germany). The cells were further stained with anti-mouse Alexa Fluor 700-conjugated anti-CD34, Pacific Blue-conjugated anti-Sca-1, and APC-conjugated anti-CD117 antibodies, as well as with APC-Cy7-conjugated streptavidin antibody for biotinylated antibodies (eBioscience). For isolation of Macrophage, BM cells from four-week-old mice were stained with an APC-conjugated anti-mouse Mac-1 (BD Biosciences) antibody. Sorting was performed on a FACSAria (Becton Dickinson, Franklin Lakes, NJ). Fetal liver cells (CD45$^-$Ter119$^-$c-Kit$^-$Dlk$^+$CD133$^+$) were prepared from E13.5 mice. Minced fetal liver tissues were dissociated with 0.05% collagenase solution and were isolated by a MoFlo^{TM} flow cytometer. Adult hepatocytes and non-parenchymal cells were isolated from postnatal livers following a 2-step collagenase digestion. Perfused liver tissues were subsequently dissociated with 0.05% collagenase solution in 10 min at 37°C. The mature-hepatocyte fraction was separated from non-parenchymal cells by several episodes of low-speed centrifugation (50 g, 1 min). Dead cell debris was removed by centrifugation in 50% Percoll solution (GE Healthcare UK, Amersham, UK). CD133+Dlk+ cells or adult hepatocytes were sorted onto feeder cells.

Induction of 2nd iPSCs

All isolated somatic cells were cultured in the presence of Dox (2 ug/ml) for induction of 2nd iPSCs. Fibroblasts and hematopoietic cells were cultured in ES/iPSC medium. FLCD45 were cultured in the presence of 10 ng/ml human TPO, 10 ng/ml mouse EPO, 10 ng/ml mouse IL-3, 10 ng/ml mouse IL-6, 10 ng/ml mouse Flt3 ligand, 10 ng/ml mouse GM-CSF, 10 ng/ml mouse VEGF and 50 ng/ml mouse SCF (Peprotech). HSCs, HPCs and MPs were cultured in the presence of 10 ng/ml human TPO, 10 ng/ml mouse IL-3, 10 ng/ml mouse IL-6 and 10 ng/ml mouse Flt3 ligand (Peprotech). Macrophages were cultured in the presence of 5 ng/ml M-CSF (Peprotech).

Liver cells were cultured in a 1:1 mixture of H-CFU-C medium (DMEM/F-12 with 10% FBS or 10% KSR, 1x Insulin-Transferrin-Selenium X, 10 mM nicotinamide, 10-7 M dexamethasone, 2.5 mM HEPES, 1x penicillin/streptomycin/L-glutamine and 1x non-essential amino acid solution and fresh DMEM/10% FBS).

Alkaline Phosphatase (ALP) Staining and Immunostaining

Alkaline phosphatase (ALP) staining was performed with Vector Red Alkaline Phosphatase Substrate Kit I (Vector Laboratories, Burlingame, CA) according to the manufacturer's instructions. 5×10^4 MEFs were infected by Ai-LV at m.o.i 0.4 and ALP positive colonies were counted 14days after infection in triplicate cultures. Efficiency of ALP positive colonies were calculated by dividing transduced cell number (2×10^4) by the number of ALP positive colonies.

Immunostaining assays were performed as follows. Cells were fixed in 4% paraformaldehyde for 10 min and washed twice with PBS. The fixed cells were incubated in MAXblocking medium (Active Motif, Carlsbad, CA) for 30 min at room temperature (RT) for blocking. The cells were then incubated with primary antibody overnight at 4°C. The day after, cells were washed with PBS and incubated with secondary antibody in PBS for 30 min at RT. Thereafter the cells were washed with PBS and 4',6 - diamidino-2-phenylindole (DAPI) was added for nuclear staining.

For iPS colony count, we performed an enzyme antibody technique by staining the cells with diaminobenzidin (DAB) solution (0.05% DAB, 50 mM Tris/HCI pH 7.4, 0.01% H_2O_2 freshly prepared) at 2weeks after seeding for miPSCs or 3weeks after seeding for riPSCs. Primary antibody used was rabbit anti-mouse Nanog antibody (ReproCELL, Kanagawa, Japan, 1:100). Secondary antibodies were Alexa Fluor 546 conjugated goat anti-rabbit IgG antibody or horseradish peroxidase (HRP) conjugated goat anti-rabbit IgG antibody (Invitrogen, Carlsbad, CA, 1:300).

RT-PCR and Quantitative PCR

Total RNA was isolated using RNAeasy kit (Qiagen, Valencia, CA) followed by cDNA synthesis using super script III reverse transcriptase (Invitrogen). PCR was performed using EX Taq HS (Takara) under the following conditions: 94°C for 1 min, followed by 30 or 35 cycles of 94°C for 30 sec, annealing temperature (from 50°C to 62°C) for 30 sec and 72°C for 30 sec, with a final extension at 72°C for 7 min. Quantitative PCR was performed using FastStart Universal SYBR Master (Roche Diagnostics, Germany) for reprogramming factors expression and iPS Efficiency Check qPCR Kit (TAKARA) for aging related gene expression. The primer sequences are listed in Table S1.

All experiments were performed under institutional guidelines.

Supporting Information

Figure S1 Phenotypic analysis of mouse and human iPSCs. (A) iPS#6 and #19 clones was differentiated by removal of MEF and Lif for two weeks and re-reprogrammed by addition of Dox. (Left; in the absence of Dox right; in the presence of Dox) (B) Proviral copy number of isolated iPS clones was analyzed by Southern blot analysis. (C) Karyotype analysis of iPS#6 clone. (D) AP staining of human iPS clone (left). Reprogramming analysis of in vitro differentiated human iPS cells in the absence of Dox (middle) and in the presence of Dox (right).
(TIF)

Figure S2 Expression profile of reprogramming genes and aging related genes in fibroblasts. (A) Expression levels of reprogramming genes (*Oct4, Klf4, Sox2* and *c-Myc*) in fibroblasts (MEF, NB fb, 1wk fb and Adult fb) compared to ESCs. (B) Expression levels of aging related genes (*p53, p21^{CIP1}, p16^{INK4a}* and *p19Arf*) in fibroblasts (MEF, NB fb, 1wk fb and Adult fb) compared to ESCs.
(TIF)

Table S1 The primer sequences for RT-PCR and Quantitative PCR.
(XLSX)

Author Contributions

Conceived and designed the experiments: TY. Performed the experiments: TY SH AK MO MK YW AU TH HS YSL MKI HM. Analyzed the data: TY. Contributed reagents/materials/analysis tools: TY SH. Wrote the paper: TY TK SY. Final approval of the manuscript: TY HN.

References

1. Takahashi K, Yamanaka S (2006) Induction of pluripotent stem cells from mouse embryonic and adult fibroblast cultures by defined factors. Cell 126: 663–676.
2. Takahashi K, Tanabe K, Ohnuki M, Narita M, Ichisaka T, et al. (2007) Induction of pluripotent stem cells from adult human fibroblasts by defined factors. Cell 131: 861–872.
3. Yu J, Vodyanik MA, Smuga-Otto K, Antosiewicz-Bourget J, Frane JL, et al. (2007) Induced pluripotent stem cell lines derived from human somatic cells. Science 318: 1917–1920.
4. Okita K, Nakagawa M, Hyenjong H, Ichisaka T, Yamanaka S (2008) Generation of mouse induced pluripotent stem cells without viral vectors. Science 322: 949–953.
5. Yu J, Hu K, Smuga-Otto K, Tian S, Stewart R, et al. (2009) Human induced pluripotent stem cells free of vector and transgene sequences. Science 324: 797–801.
6. Kaji K, Norrby K, Paca A, Mileikovsky M, Mohseni P, et al. (2009) Virus-free induction of pluripotency and subsequent excision of reprogramming factors. Nature 458: 771–775.
7. Yusa K, Rad R, Takeda J, Bradley A (2009) Generation of transgene-free induced pluripotent mouse stem cells by the piggyBac transposon. Nat Methods 6: 363–369.
8. Yakubov E, Rechavi G, Rozenblatt S, Givol D (2010) Reprogramming of human fibroblasts to pluripotent stem cells using mRNA of four transcription factors. Biochem Biophys Res Commun 394: 189–193.
9. Warren L, Manos PD, Ahfeldt T, Loh YH, Li H, et al. (2010) Highly efficient reprogramming to pluripotency and directed differentiation of human cells with synthetic modified mRNA. Cell Stem Cell 7: 618–630.
10. Cho HJ, Lee CS, Kwon YW, Paek JS, Lee SH, et al. (2010) Induction of pluripotent stem cells from adult somatic cells by protein-based reprogramming without genetic manipulation. Blood 116: 386–395.
11. Sommer CA, Stadtfeld M, Murphy GJ, Hochedlinger K, Kotton DN, et al. (2009) Induced pluripotent stem cell generation using a single lentiviral stem cell cassette. Stem Cells 27: 543–549.
12. Carey BW, Markoulaki S, Hanna J, Saha K, Gao Q, et al. (2009) Reprogramming of murine and human somatic cells using a single polycistronic vector. Proc Natl Acad Sci U S A 106: 157–162.
13. Stadtfeld M, Nagaya M, Utikal J, Weir G, Hochedlinger K (2008) Induced pluripotent stem cells generated without viral integration. Science 322: 945–949.
14. Fusaki N, Ban H, Nishiyama A, Saeki K, Hasegawa M (2009) Efficient induction of transgene-free human pluripotent stem cells using a vector based on Sendai virus, an RNA virus that does not integrate into the host genome. Proc Jpn Acad Ser B Phys Biol Sci 85: 348–362.
15. Ban H, Nishishita N, Fusaki N, Tabata T, Saeki K, et al. (2011) Efficient generation of transgene-free human induced pluripotent stem cells (iPSCs) by temperature-sensitive Sendai virus vectors. Proc Natl Acad Sci U S A 108: 14234–14239.
16. Carey BW, Markoulaki S, Beard C, Hanna J, Jaenisch R (2010) Single-gene transgenic mouse strains for reprogramming adult somatic cells. Nat Methods 7: 56–59.
17. Stadtfeld M, Maherali N, Borkent M, Hochedlinger K (2010) A reprogrammable mouse strain from gene-targeted embryonic stem cells. Nat Methods 7: 53–55.
18. McMahon SB, Van Buskirk HA, Dugan KA, Copeland TD, Cole MD (1998) The novel ATM-related protein TRRAP is an essential cofactor for the c-Myc and E2F oncoproteins. Cell 94: 363–374.
19. Martinato F, Cesaroni M, Amati B, Guccione E (2008) Analysis of Myc-induced histone modifications on target chromatin. PLoS One 3: e3650.
20. Nakagawa M, Koyanagi M, Tanabe K, Takahashi K, Ichisaka T, et al. (2008) Generation of induced pluripotent stem cells without Myc from mouse and human fibroblasts. Nat Biotechnol 26: 101–106.
21. Nakagawa M, Takizawa N, Narita M, Ichisaka T, Yamanaka S (2010) Promotion of direct reprogramming by transformation-deficient Myc. Proc Natl Acad Sci U S A 107: 14152–14157.
22. Araki R, Hoki Y, Uda M, Nakamura M, Jincho Y, et al. (2011) Crucial role of c-Myc in the generation of induced pluripotent stem cells. Stem Cells 29: 1362–1370.
23. Polo JM, Liu S, Figueroa ME, Kulalert W, Eminli S, et al. (2010) Cell type of origin influences the molecular and functional properties of mouse induced pluripotent stem cells. Nat Biotechnol 28: 848–855.
24. Hu Q, Friedrich AM, Johnson LV, Clegg DO (2010) Memory in induced pluripotent stem cells: reprogrammed human retinal-pigmented epithelial cells show tendency for spontaneous redifferentiation. Stem Cells 28: 1981–1991.
25. Kim K, Doi A, Wen B, Ng K, Zhao R, et al. (2010) Epigenetic memory in induced pluripotent stem cells. Nature 467: 285–290.
26. Huangfu D, Osafune K, Maehr R, Guo W, Eijkelenboom A, et al. (2008) Induction of pluripotent stem cells from primary human fibroblasts with only Oct4 and Sox2. Nat Biotechnol 26: 1269–1275.
27. Huangfu D, Maehr R, Guo W, Eijkelenboom A, Snitow M, et al. (2008) Induction of pluripotent stem cells by defined factors is greatly improved by small-molecule compounds. Nat Biotechnol 26: 795–797.
28. Hamanaka S, Yamaguchi T, Kobayashi T, Kato-Itoh M, Yamazaki S, et al. (2011) Generation of germline-competent rat induced pluripotent stem cells. PLoS One 6: e22008.
29. Kobayashi T, Yamaguchi T, Hamanaka S, Kato-Itoh M, Yamazaki Y, et al. (2010) Generation of rat pancreas in mouse by interspecific blastocyst injection of pluripotent stem cells. Cell 142: 787–799.
30. Papapetrou EP, Tomishima MJ, Chambers SM, Mica Y, Reed E, et al. (2009) Stoichiometric and temporal requirements of Oct4, Sox2, Klf4, and c-Myc expression for efficient human iPSC induction and differentiation. Proc Natl Acad Sci U S A 106: 12759–12764.
31. Banito A, Rashid ST, Acosta JC, Li S, Pereira CF, et al. (2009) Senescence impairs successful reprogramming to pluripotent stem cells. Genes Dev 23: 2134–2139.
32. Sridharan R, Tchieu J, Mason MJ, Yachechko R, Kuoy E, et al. (2009) Role of the murine reprogramming factors in the induction of pluripotency. Cell 136: 364–377.
33. Marion RM, Blasco MA (2010) Telomeres and telomerase in adult stem cells and pluripotent embryonic stem cells. Adv Exp Med Biol 695: 118–131.
34. Kleger A, Mahaddalkar P, Katz SF, Lechel A, Ju JY, et al. (2012) Increased Reprogramming Capacity of Mouse Liver Progenitor Cells, Compared With Differentiated Liver Cells, Requires the BAF Complex. Gastroenterology.
35. Shibuya K, Shirakawa J, Kameyama T, Honda S, Tahara-Hanaoka S, et al. (2003) CD226 (DNAM-1) is involved in lymphocyte function-associated antigen 1 costimulatory signal for naive T cell differentiation and proliferation. J Exp Med 198: 1829–1839.
36. Matsumoto K, Isagawa T, Nishimura T, Ogaeri T, Eto K, et al. (2009) Stepwise development of hematopoietic stem cells from embryonic stem cells. PLoS One 4: e4820.

— 199 —

PLoS one

Bmi1 Confers Resistance to Oxidative Stress on Hematopoietic Stem Cells

Shunsuke Nakamura[1,4], Motohiko Oshima[1,4], Jin Yuan[1,4], Atsunori Saraya[1,4], Satoru Miyagi[1,4], Takaaki Konuma[1], Satoshi Yamazaki[2,5], Mitsujiro Osawa[1,4], Hiromitsu Nakauchi[2,5], Haruhiko Koseki[3,4], Atsushi Iwama[1,4]*

1 Department of Cellular and Molecular Medicine, Graduate School of Medicine, Chiba University, Chiba, Japan, 2 Division of Stem Cell Therapy, Center for Stem Cell Biology and Regenerative Medicine, Institute of Medical Science, University of Tokyo, Tokyo, Japan, 3 RIKEN Research Center for Allergy and Immunology, Yokohama, Japan, 4 Japan Science and Technology Agency (JST), CREST, Tokyo, Japan, 5 ERATO, Chiyoda-ku, Tokyo, Japan

Abstract

Background: The polycomb-group (PcG) proteins function as general regulators of stem cells. We previously reported that retrovirus-mediated overexpression of *Bmi1*, a gene encoding a core component of polycomb repressive complex (PRC) 1, maintained self-renewing hematopoietic stem cells (HSCs) during long-term culture. However, the effects of overexpression of *Bmi1* on HSCs *in vivo* remained to be precisely addressed.

Methodology/Principal findings: In this study, we generated a mouse line where *Bmi1* can be conditionally overexpressed under the control of the endogenous *Rosa26* promoter in a hematopoietic cell-specific fashion (*Tie2-Cre;R26Stop^{FL}Bmi1*). Although overexpression of *Bmi1* did not significantly affect steady state hematopoiesis, it promoted expansion of functional HSCs during *ex vivo* culture and efficiently protected HSCs against loss of self-renewal capacity during serial transplantation. Overexpression of *Bmi1* had no effect on DNA damage response triggered by ionizing radiation. In contrast, *Tie2-Cre;R26Stop^{FL}Bmi1* HSCs under oxidative stress maintained a multipotent state and generally tolerated oxidative stress better than the control. Unexpectedly, overexpression of *Bmi1* had no impact on the level of intracellular reactive oxygen species (ROS).

Conclusions/Significance: Our findings demonstrate that overexpression of *Bmi1* confers resistance to stresses, particularly oxidative stress, onto HSCs. This thereby enhances their regenerative capacity and suggests that Bmi1 is located downstream of ROS signaling and negatively regulated by it.

Introduction

Hematopoietic stem cells (HSCs) are defined as primitive cells that are capable of both self-renewal and differentiation into any of the hematopoietic cell lineages. Cell fate decisions of HSCs (self-renewal vs. differentiation) are precisely regulated to maintain their numbers and lifespan. Defects in these processes lead to hematopoietic insufficiencies and to the development of hematopoietic malignancies.

The polycomb-group (PcG) proteins play key roles in the initiation and maintenance of gene silencing through histone modifications. PcG proteins belong to two major complexes, Polycomb repressive complex 1 and 2 (PRC1 and PRC2). PRC1 monoubiquitylates histone H2A at lysine 119 and PRC2 trimethylates histone H3 at lysine 27 [1]. Of note, PcG proteins have been implicated in the maintenance of self-renewing stem cells [2–4]. Among PcG proteins, Bmi1, a core component of

PRC1, plays an essential role in the maintenance of self-renewal ability of HSCs at least partially by silencing the *Ink4a/Arf* locus [5–8]. Bmi1 also maintains multipotency of HSCs by keeping developmental regulator gene promoters poised for activation [9]. Furthermore, Bmi1 has been implicated in the maintenance of the proliferative capacity of leukemic stem cells [5]. Consistent with these findings, levels of BMI1 expression in the human CD34+ cell fraction have been reported to correlate well with the progression and prognosis of myelodysplastic syndrome and chronic and acute myeloid leukemia [4,10], suggesting a role of BMI1 in leukemic stem cells.

We previously reported that overexpression of *Bmi1* using a retrovirus maintains self-renewal capacity of HSCs and markedly expands multipotent progenitors *ex vivo*, resulting in an enhancement of repopulating capacity of HSCs after culture. Likewise, forced expression of *BMI1* was demonstrated to promote leukemic transformation of human CD34+ cells by *BCR-ABL* [11].

— 200 —

However, the effects of overexpression of *Bmi1* on hematopoiesis remained to be precisely addressed.

In this study, we generated mice overexpressing *Bmi1* in a hematopoietic cell-specific manner. We analyzed the effects of overexpression of *Bmi1* on hematopoiesis under steady state conditions as well as under multiple stresses. Our findings revealed a protective function for Bmi1 in HSCs from stresses, such as ROS, that usually limit the lifespan of HSCs.

Results

Generation of Mice Overexpressing *Bmi1* in Hematopoietic Cells

To generate tissue-specific *Bmi1*-transgenic mice, we knocked a loxP-flanked neo^r-stop cassette followed by Flag-tagged *Bmi1*, an frt-flanked *IRES-eGFP* cassette, and a bovine polyadenylation sequence into the *Rosa26* locus (**Figure 1A**). The obtained mice (hereafter referred to as *R26Stop^{FL}Bmi1*) were crossed with *Tie2-Cre* mice [12] to drive *Bmi1* expression in a hematopoietic cell-specific manner. Quantitative RT-PCR analysis of bone marrow (BM) Lineage marker Sca-1$^+$c-Kit$^+$ (LSK) cells confirmed 6-fold over-expression of *Bmi1* in *Tie2-Cre;R26Stop^{FL}Bmi1* mice compared to the *Tie2-Cre* control mice (**Figure 1B**). Western blot analysis also verified overexpression of Bmi1 protein in BM c-Kit$^+$ progenitor cells from *Tie2-Cre;R26Stop^{FL}Bmi1* mice (**Figure 1C**).

Steady State Hematopoiesis in *Tie2-Cre;R26Stop^{FL}Bmi1* Mice

We first investigated the effect of overexpression of *Bmi1* on hematopoiesis in a steady state. Unexpectedly, 10-week-old *Tie2-Cre;R26Stop^{FL}Bmi1* mice did not exhibit any significant differences in the numbers of total BM cells, CD34 LSK HSCs, LSK cells, multipotent progenitors (MPPs), common myeloid progenitors (CMPs), granulocyte/macrophage progenitors (GMPs), megakaryocyte/erythroid progenitors (MEPs), or common lymphoid progenitors (CLPs) compared to the *Tie2-Cre* control mice (**Figure 1D** and **Figure S1A**). The number of white blood cells (WBC) in peripheral blood (PB) did not change upon forced expression of *Bmi1*. Only the proportion of PB Gr-1$^+$/Mac-1$^+$ myeloid cells in *Tie2-Cre;R26Stop^{FL}Bmi1* mice was significantly higher than in the control mice, although the difference was not drastic (a difference of only about 2%) (**Figure 1D**). Furthermore, *Tie2-Cre;R26Stop^{FL}Bmi1* mice did not show any significant differences in the numbers of total spleen cells, LSK cells in the spleen, total thymic cells, or CD4$^+$CD8$^-$, CD4$^-$CD8$^+$, or CD4$^+$CD8$^+$ cells in the thymus compared to the control mice (**Figure S1A**). These findings indicate that overexpression of *Bmi1* does not largely compromise differentiation of HSCs. We further analyzed the cell cycle status of CD34 LSK HSCs by Pyronin Y staining, but again did not detect any changes (**Figure S1B**). These results indicate that overexpression of *Bmi1* only slightly perturbs hematopoiesis under steady state conditions, suggesting that the level of endogenous Bmi1 is sufficient to repress the transcription of its target genes.

Colony-forming Capacity of Hematopoietic Stem and Progenitor Cells Overexpressing *Bmi1*

We next evaluated the proliferative and differentiation capacity of *Tie2-Cre;R26Stop^{FL}Bmi1* HSCs *in vitro*. Single CD34 LSK HSCs were clonally sorted into 96-microtiter plates with the medium supplemented with stem cell factor (SCF), thrombopoietin (TPO), interleukin-3 (IL-3), and erythropoietin (EPO) and allowed to form colonies. At day 14 of culture, the colonies were counted and individually collected for morphological examination. Both *Tie2-Cre* control and *Tie2-Cre;R26Stop^{FL}Bmi1* HSCs gave rise to comparable numbers of high proliferative potential (HPP) and low proliferative potential (LPP) colonies with a diameter greater than and less than 1 mm, respectively (**Figure 2A**). The morphological analysis of colonies revealed that the number of colony-forming unit (CFU)-neutrophil/macrophage/erythroblast/megakaryocyte (nmEM) was also comparable between the two groups (**Figure 2A**). CFU-nmEM is a major subpopulation among CD34$^-$LSK HSCs and its frequency is well correlated with that of functional HSCs [13]. These findings indicate that overexpression of *Bmi1* in freshly isolated CD34 LSK HSCs does not affect their colony-forming capacity or differentiation *in vitro*.

We previously reported that overexpression of *Bmi1* by retroviral transduction efficiently maintains hematopoietic stem and progenitor cells during long-term culture [7]. We re-evaluated the effect of forced expression of *Bmi1* using *Tie2-Cre;R26-Stop^{FL}Bmi1* HSCs. CD34 LSK cells were cultured for 10 days in a serum-free medium supplemented with SCF and TPO, a cytokine combination which supports the proliferation of HSCs and progenitors rather than their differentiation [14]. Although *Tie2-Cre;R26Stop^{FL}Bmi1* HSCs did not show any growth advantage over the control (**Figure 2B**), the *Tie2-Cre;R26Stop^{FL}Bmi1* HSC culture contained significantly more HPP-colony-forming cells (CFCs) and CFU-nmEM than the control (**Figure 2B**). Correspondingly, flow cytometric analysis revealed more LSK cells in the *Tie2-Cre;R26Stop^{FL}Bmi1* HSC culture than in the control culture at day 14 (**Figure 2C**). There was no significant difference in the frequency of apoptotic cells between the control and *Tie2-Cre;R26Stop^{FL}Bmi1* HSC cultures (**Figure S2A**). Of note, however, the *Tie2-Cre;R26Stop^{FL}Bmi1* HSC culture contained a significantly higher proportion of LSK cells in the G_0/G_1 stage of cell cycle than the control (**Figure S2B**). These findings suggest that overexpression of *Bmi1* slows down cell cycle of immature hematopoietic cells in culture, leading to no growth advantages over the control cells in spite of an increase in immature progenitors in culture. As we reported previously, the *Ink4a/Arf* locus is a critical target of Bmi1 in HSCs [8]. Quantitative RT-PCR confirmed that *p19^{Arf}* was closely repressed in transcription upon *Bmi1* overexpression (**Figure 2D**). These results support our previous finding that HSCs overexpressing *Bmi1* retain their self-renewal capacity better than the control HSCs under the culture stress.

Overexpression of *Bmi1* Enhances Expansion of HSCs *ex vivo* and Protects HSCs During Serial Transplantation

HSCs are exposed to oxidative stress during long-term culture in 20% O_2 [15]. In order to precisely determine the effect of overexpression of *Bmi1* on HSCs during culture, we next determined the frequency of functional HSCs contained in optimized serum-free culture by competitive repopulating unit (CRU) assay. We first transplanted limiting doses of fresh CD34 LSK cells from *Tie2-Cre* and *Tie2-Cre;R26Stop^{FL}Bmi1* mice along with 2×10^5 competitor BM cells. The frequency of long-term repopulating HSCs was 1 in 8 among fresh CD34 LSK cells from both *Tie2-Cre* and *Tie2-Cre;R26Stop^{FL}Bmi1* mice (**Figure 3**). We then cultured CD34 LSK cells for 10 days in a serum-free medium supplemented with SCF and TPO in 20% O_2. During the 10-day culture period, functional HSCs increased 4-fold (1 out of 2 CD34 LSK cells) in control CD34 LSK cells. Interestingly, overexpression of *Bmi1* established 2-fold better expansion of HSCs than the control during culture *ex vivo* (**Figure 3**). These findings are the first to show that Bmi1 has a role in the expansion of HSCs.
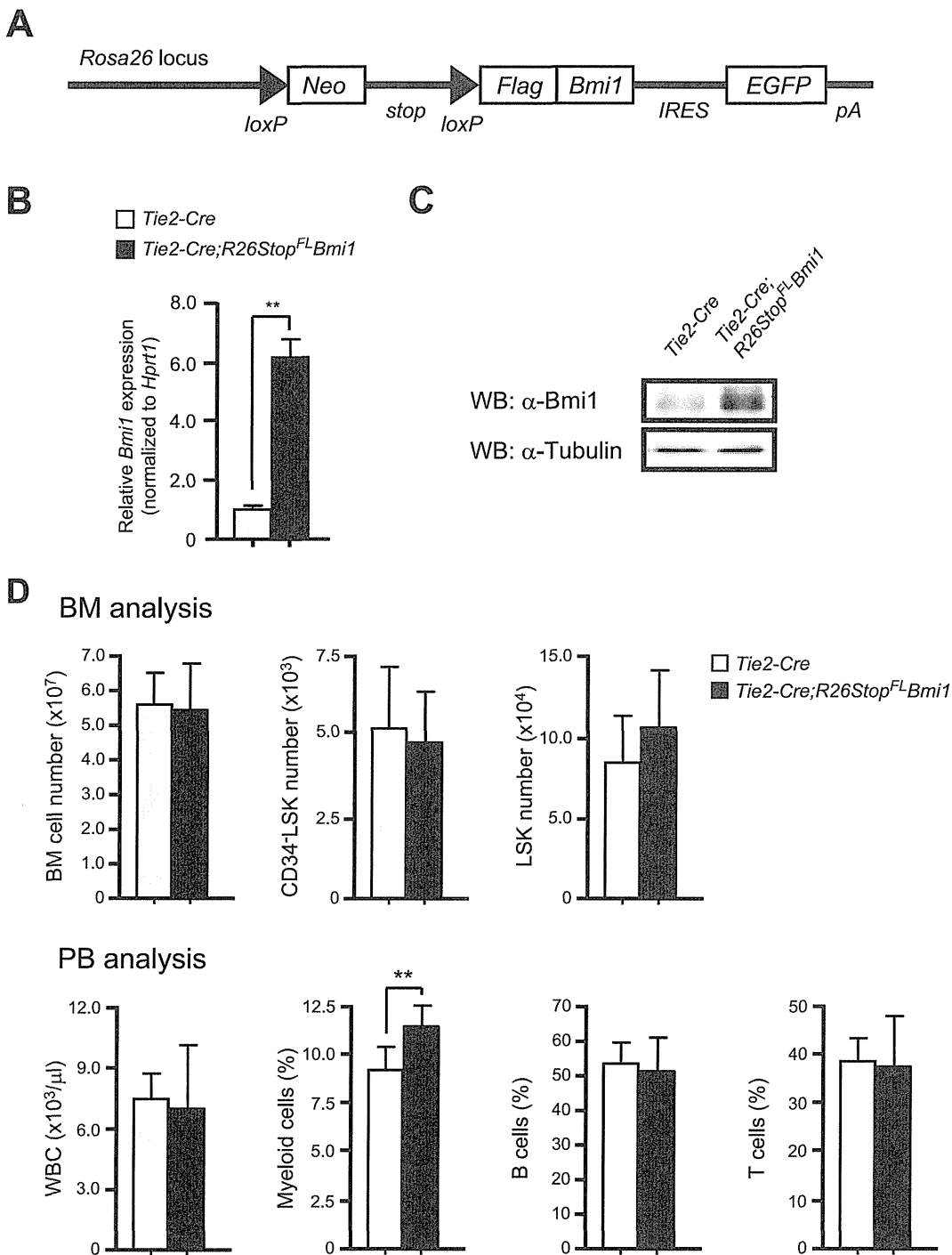
— 201 —

Figure 1. Generation of mice overexpressing *Bmi1* **in hematopoietic cells.** (A) Strategy for making a knock-in allele for *Bmi1* downstream of the *Rosa26* promoter. A *loxP*-flanked *neo*^{r}-stop cassette followed by Flag-tagged *Bmi1*, an *frt*-flanked *IRES-eGFP* cassette, and a bovine polyadenylation sequence was knocked-in the *Rosa26* locus. (B) Quantitative RT-PCR analysis of *Bmi1* in BM LSK cells from *Tie2-Cre* and *Tie2-Cre;R26Stop*^{FL}*Bmi1* mice. mRNA levels were normalized to *Hprt1* expression. Expression levels relative to that in *Tie2-Cre* LSK cells are shown as the mean ± S.D. (n = 3). (C) Western blotting analysis of Bmi1 in c-Kit$^+$ BM cells from *Tie2-Cre* and *Tie2-Cre;R26Stop*^{FL}*Bmi1* mice. α-tubulin was used as the loading control. (D) Hematopoietic analysis of 10-week-old *Tie2-Cre* and *Tie2-Cre;R26Stop*^{FL}*Bmi1* mice. Absolute numbers of BM cells, CD34⁻LSK cells, and LSK cells in bilateral femurs and tibiae are presented as the mean ± S.D. (upper panels, *Tie2-Cre*; n = 7, *Tie2-Cre;R26Stop*^{FL}*Bmi1*; n = 8). PB analysis of 10-week-old *Tie2-Cre* and *Tie2-Cre;R26Stop*^{FL}*Bmi1* mice. White blood cell (WBC) counts and lineage contribution of myeloid, B, and T cells are shown as the mean ± S.D. (lower panels, *Tie2-Cre*; n = 7, *Tie2-Cre;R26Stop*^{FL}*Bmi1*; n = 8). ** $p<0.01$.
doi:10.1371/journal.pone.0036209.g001

HSCs are exposed to various stresses including replicative and oxidative stresses during serial transplantation and eventually lose self-renewal capacity [16,17]. We hypothesized that the effects of overexpression of *Bmi1* on HSCs would manifest under stressful conditions such as serial transplantations. Therefore, we performed competitive repopulation assays using 5×10^5 fresh BM
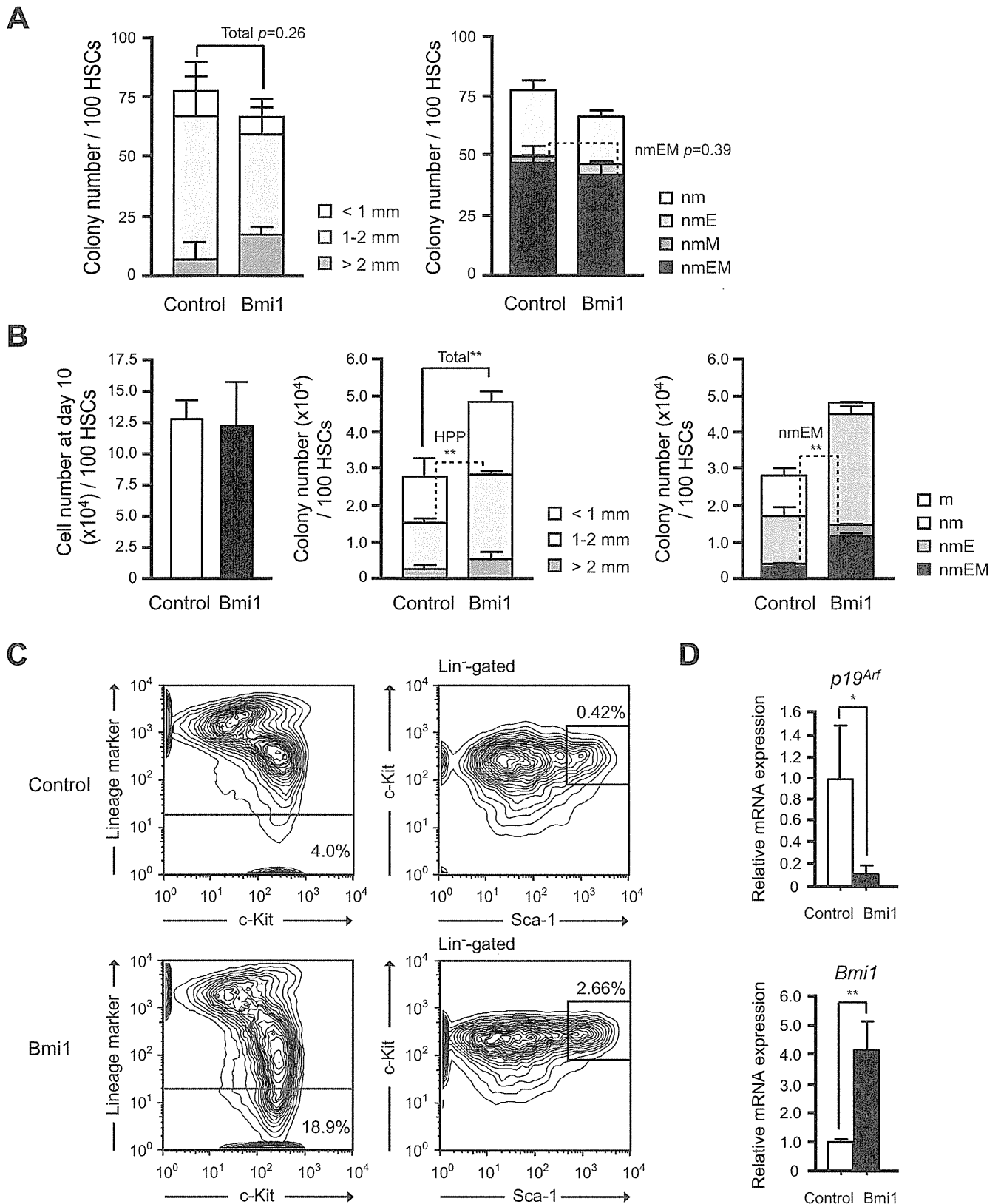
Figure 2. Effects of overexpression of *Bmi1* on HSCs *in vitro*. (A) Colony formation by HSCs isolated from *Tie2-Cre* (Control) and *Tie2-Cre;R26Stop^FL^Bmi1* (Bmi1) mice. Single CD34⁻LSK cells were sorted into 96-well microtiter plates containing the SF-O3 medium supplemented with 10% FBS and multiple cytokines (10 ng/ml SCF, 10 ng/ml TPO, 10 ng/ml IL-3, and 3 u/ml EPO) and allowed to form colonies. At day 14 of culture, the colonies were counted and individually collected for morphological examination. Absolute numbers of LPP and HPP-CFCs which gave rise to colonies with a diameter less and greater than 1 mm, respectively are shown as the mean ± S.D. for triplicate cultures (left panel). Absolute numbers of each

colony types were defined by the composition of colonies (right panel). Colonies were recovered and examined by microscopy to determine colony types. Composition of colonies is depicted as n, neutrophils; m, macrophages; E, erythroblasts; and M, megakaryocytes. (B) Colony formation by HSCs cultured for 10 days. CD34⁻LSK cells from *Tie2-Cre* (Control) and *Tie2-Cre;R26Stop^{FL}Bmi1* (Bmi1) mice were cultured in the SF-O3 serum-free medium supplemented with 50 ng/ml of SCF and TPO. At day 10 of culture, the cells were counted (left panel) and plated in methylcellulose medium to allow formation of colonies in the presence of 20 ng/ml SCF, 20 ng/ml TPO, 20 ng/ml IL-3, and 3 u/ml EPO. Absolute numbers of LPP and HPP-CFCs (middle panel) are shown as the mean ± S.D. for triplicate cultures. Absolute numbers of each colony type are shown in the right panel. (C) Flow cytometric analysis of CD34⁻LSK HSCs at day14 of culture. Representative flow cytometric profiles of LSK cells in cultures of CD34⁻LSK HSCs from *Tie2-Cre* (Control) and *Tie2-Cre;R26Stop^{FL}Bmi1* (Bmi1) mice are depicted. The proportion of Lin⁻ and LSK cells in total cells are indicated. (D) Quantitative RT-PCR analysis of the expression of $p19^{Arf}$, and *Bmi1* in *Tie2-Cre* (Control) and *Tie2-Cre;R26Stop^{FL}Bmi1* (Bmi1) LSK cells. LSK cells were purified by cell sorting from CD34⁻LSK cultures in (C) at day 14 of culture. Each value was normalized to *Hprt1* expression and the expression level of each gene in control cells was arbitrarily set to 1. Data are shown as the mean ± S.D. for triplicate analyses. * $p<0.05$, ** $p<0.01$.
doi:10.1371/journal.pone.0036209.g002

cells along with 5×10^5 competitor BM cells (**Figure 4A**) or the total cells produced from 20 CD34⁻LSK cells after a 10-day culture period along with 2×10^5 competitor BM cells (**Figure 4B**). The flow cytometric analysis of PB revealed little or no difference in the chimerism of donor cells between *Tie2-Cre* and *Tie2-Cre;R26Stop^{FL}Bmi1* cells at 12 weeks after the primary transplantations. However, in the secondary and tertiary transplantations, the chimerism of *Tie2-Cre* cells significantly declined while that of *Tie2-Cre;R26Stop^{FL}Bmi1* cells drasticaly increased. *Tie2-Cre* cells

after 10-day culture failed to reconstitute hematopoiesis in the quaternary transplantation, while *Tie2-Cre;R26Stop^{FL}Bmi1* cells still established robust repopulation (**Figure 4B**). The chimerism of donor cells in BM LSK cells mirrored the changes in the PB. These results clearly indicate that overexpression of *Bmi1* protects HSCs against the loss of self-renewal capacity during serial transplantation. The findings thus far suggest that overexpression of *Bmi1* confers stress resistance onto HSCs.

Summary of % of engrafted mice and frequency of HSCs in CRU assays

	Number of CD34⁻LSK cells injected							Frequency	95% CI
	0.5	1	1.5	2	5	10	20		
Fresh control				1/9	4/10	7/10	6/6	1/8	1/14~1/5
Fresh Bmi1				1/10	6/10	6/10	5/5	1/8	1/13~1/5
Cultured control	1/7	4/7	3/8	7/10	10/10	9/9		1/2	1/3~1/1
Cultured Bmi1	5/7	6/7	8/8	8/10	9/10	10/10		1/1	1/2~1/1

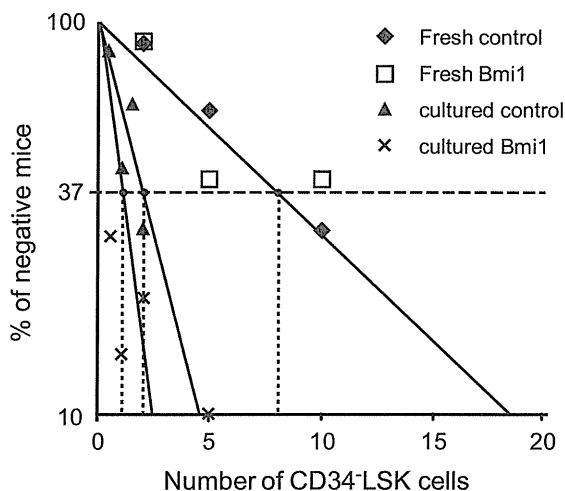*** (between Cultured control 1/2 and Cultured Bmi1 1/1)

Figure 3. Overexpression of *Bmi1* enhances expansion of HSCs *ex vivo*. Competitive repopulating unit (CRU) assays using limiting numbers of CD34⁻LSK cells from *Tie2-Cre* (Control) mice and *Tie2-Cre;R26Stop^{FL}Bmi1* (Bmi1) mice. Freshly isolated CD34⁻LSK cells were immediately used for BM transplantation, or CD34⁻LSK cells were cultured in the SF-O3 serum-free medium supplemented with 50 ng/ml SCF and TPO for 10 days, and then a fraction of the culture cells corresponding to the indicated number (0.5~10) of initial CD34⁻LSK cells was subjected to BM transplantation. The test cells (CD45.2) were transplanted along with 2×10^5 competitor BM cells (CD45.1) into CD45.1 recipient mice lethally irradiated at a dose of 9.5 Gy. Percent chimerism of donor cells in the recipient PB was determined at 16 weeks after transplantation. The mice with chimerism more than 1% in all three lineages (myeloid, B, and T cells) were considered successfully engrafted and the others were defined as negative mice. The frequency of HSCs was calculated using L-Calc software. The proportion of engrafted mice, frequency of functional HSCs, and the 95% confidence interval (CI) are summarized in the table and each data is plotted in the bottom panel. *** $p<0.001$.
doi:10.1371/journal.pone.0036209.g003

— 204 —